JAERI-Review
2005-005

REVIEW OF JAERI ACTIVITIES ON THE IFMIF LIQUID LITHIUM TARGET IN FY2004

March 2005

Hiroo NAKAMURA, Mizuho IDA, Kenjiro MATSUHIRO,
Ulrich FISCHER*, Takumi HAYASHI, Seiji MORI*,
Hirofumi NAKAMURA, Takeo NISHITANI, Katsusuke SHIMIZU*,
Stanislav SIMAKOV*, Masayoshi SUGIMOTO, Morio TAKEMURA,
Toshio YAMAMURA* and Michinori YAMAUCHI

日本原子力研究所
Japan Atomic Energy Research Institute

本レポートは、日本原子力研究所が不定期に公刊している研究報告書です。
入手の問合わせは、日本原子力研究所研究情報部研究情報課(〒319-1195 茨城県那珂郡東海村)あて、お申し越し下さい。なお、このほかに財団法人原子力弘済会資料センター(〒319-1195 茨城県那珂郡東海村日本原子力研究所内)で複写による実費頒布を行っております。

This report is issued irregularly.
Inquiries about availability of the reports should be addressed to Research Information Division, Department of Intellectual Resources, Japan Atomic Energy Research Institute, Tokai-mura, Naka-gun, Ibaraki-ken 〒319-1195, Japan.

編集兼発行　日本原子力研究所

JAERI－Review 2005－005

Review of JAERI Activities on the IFMIF Liquid Lithium Target in FY2004

Hiroo NAKAMURA, Mizuho IDA※1, Kenjiro MATSUHIRO※3, Ulrich FISCHER*1, Takumi HAYASHI, Seiji MORI*2, Hirofumi NAKAMURA, Takeo NISHITANI, Katsusuke SHIMIZU*3, Stanislav SIMAKOV*1,Masayoshi SUGIMOTO, Morio TAKEMURA※2, Toshio YAMAMURA*4 and Michinori YAMAUCHI※1

Department of Fusion Engineering Research
(Tokai Site)
Naka Fusion Research Establishment
Japan Atomic Energy Research Institute
Tokai-mura, Naka-gun, Ibaraki-ken

(Received January 26,2005)

The International Fusion Materials Irradiation Facility (IFMIF) is being jointly planned to provide an accelerator-based Deuterium-Lithium (Li) neutron source to produce intense high energy neutrons (2 MW/m^2) up to 200 dpa and a sufficient irradiation volume (500 cm^3) for testing the candidate materials and components up to about a full lifetime of their anticipated use in ITER and DEMO. To realize such a condition, 40 MeV deuteron beam with a current of 250 mA is injected into high speed liquid Li flow with a speed of 20 m/s. In target system, radioactive species such as ^7Be, tritium and activated corrosion products are generated. In addition, back wall operates under severe conditions of neutron irradiation damage (about 50 dpa/y). In this paper, the thermal and thermal stress analyses, the accessibility evaluation of the IFMIF Li loop, and the tritium inventory and permeation of the IFMIF Li loop are summarized as JAERI activities on the IFMIF target system performed in FY2004.

Keywords: IFMIF, Fusion Material, Neutron Irradiation, Liquid Lithium Target, Thermal Stress, Neutron Activation, Dose Rate, Tritium Inventory, Permeation

---

※1 Cooperative Stuff
※2 Cooperative Stuff (Department of ITER Project)
※3 Post-Doctoral Fellow
＊1 Forschungszentrum Karlsruhe, Association FZK-Euratom,Germany
＊2 Kawasaki Heavy Industries, LTD.
＊3 Mitsubishi Heavy Industries, Ltd.
＊4 Ishikawajima-Harima Heavy Industries, Co., Ltd.

IFMIF液体リチウムターゲットに関する平成１６年度の原研の活動

日本原子力研究所那珂研究所核融合工学部
中村　博雄・井田　瑞穂※1・松廣　健二郎※3・Ulrich FISCHER*1・林　巧
森　清治*2・中村　博文・西谷　健夫・清水　克祐*3・Stanislav SIMAKOV*1
杉本　昌義・竹村　守雄※2・山村外志夫*4・山内　通則※1

（2005年1月26日受理）

国際核融合材料照射施設(IFMIF)は、核融合炉材料の開発のために、十分な照射体積（500 cm3）を有し照射量200 dpaまで照射可能な強力中性子束（2 MW/m^2）を発生可能な加速器型中性子源である。このような中性子を発生させるために、最大エネルギー40 MeV、最大電流250 mAの重水素ビームを、最大流速20 m/sの液体リチウム流ターゲットに入射させる。ターゲット系では、^{7}Be、トリチウムや放射化腐食生成物等が発生する。また、背面壁は、年間50 dpaの中性子照射下で使用する必要が有る。本報告では、平成１６年度の原研におけるターゲット系の活動での主要なトピックスとして、ターゲットアセンブリの熱・熱応力解析、放射化腐食生成物によるリチウムループ近接性の影響評価、トリチウムインベントリと透過量評価を取りまとめた。

那珂研究所（東海駐在）：〒319-1195　茨城県那珂郡東海村白方白根2-4
※1 業務協力員
※2 業務協力員（ITER 安全設計室）
※3 博士研究員
＊1 カールスルーヘ中央研究機構、ドイツ連邦共和国
＊2 川崎重工業株式会社
＊3 三菱重工業株式会社
＊4 石川島播磨重工業株式会社

Contents

目 次

1. Introduction

The IFMIF is an accelerator-based Deuterium-Lithium (Li) neutron source to produce intense high energy neutrons (2 MW/m^2) up to 200 dpa in a sufficient irradiation volume (500 cm^3) for testing candidate materials and components used in ITER and DEMO reactor [1]. To realize such a condition, a 40 MeV deuteron beam with a current of 250 mA is injected into a Li target assembly where liquid Li circulates.

For removing heat of the beams and ensuring the intense neutron field, stability of high-speed free-surface Li flow along a concave backwall is necessary. Among the assembly, the backwall is located in the most severe region of neutron irradiation. Thermal deformation of the backwall due to nuclear heating by neutron is a critical issue for maintaining the stability of Li flow.

Neutrons are produced in the Li flow and emitted through a back wall to high flux test module. Since, the back wall will be activated under intense irradiation of about 50 dpa/year, replacement of Li target assembly including the back wall is performed by a remote handling system. However, activated materials of the back wall are transferred into the Li flow due to erosion/corrosion process and deposit on inner surface of the Li loop components. Therefore, accessibility around the Li loop piping will depend on a radiation dose rate caused by the deposition of the activated materials. The accessibility evaluation of the IFMIF Li loop needs to be done considering the deposition of the activated corrosion products.

In the IFMIF, tritium is generated in the Li flow. Most of the generated tritium is removed by an yttrium hot trap in a Li purification loop, where impurities in the liquid Li are removed. However, a part of the tritium remains in the Li loop, and permeates through the wall of the Li loop components. The permeated tritium is released to the Li loop area filled with Ar gas or to test cell area. It is important for the safety of the IFMIF to evaluate the amount of tritium permeation and inventory in the Li loop of the IFMIF target system.

In this paper, JAERI activities on target system performed in FY2004 are summarised. Major topics are the thermal and thermal stress analyses of the backwall and thermal shielding / insulation around the target assembly, the accessibility evaluation of the IFMIF Li loop, and the tritium inventory and permeation of the IFMIF Li loop.

Reference

[1-1] Moeslang,A., Fischer,U., Heizel,V., Vladimirov,P., et al., "Recent Advances at the International Fusion Materials Irradiation Facility IFMIF", 19th Fusion Energy Conference, 14-19, Oct.2002, Lyon (IAEA-CN-94/FT/1-2).

2. Liquid Lithium Target in IFMIF

2.1 Li Target Facility

The Target Facility is one of the major facilities of IFMIF[2-1],[2-2]. The major function of the Li target system is to provide a stable Li jet for production of intense neutrons under irradiation of a 10 MW deuterium beam. The averaged surface heat flux on the free liquid Li flow is 1 GW/m^2. To handle such an ultra high heat load, a high speed liquid Li jet flow of 20 m/s is necessary. The system consists of a target assembly, a Li main loop, a Li purification system and a heat exchange system. Table 2-1 summarizes the major design requirements of the target facility based on these results. A block diagram of the Li target system is shown in Fig.2-1. The Li loop circulates the liquid Li to and from the target assembly through a Li purification and heat exchange system by an electromagnetic pump. The Li purification system, with a cold trap and two hot traps, is able to maintain tritium, ^{7}Be, radioactive corrosion products and other impurities under permissible levels to realize the required safety condition and to minimize corrosion of the loop materials.

2.2 Target Assembly

The target assembly is made of stainless steel 316, except for the back wall, which will use either Reduced-Activation Ferritic/Martensitic (RAFM) steel or stainless steel 316. The back wall operates under severe conditions of neutron irradiation damage (about 50 dpa/y); therefore, the back wall is designed for replacement every 11 months. Two design options for the back wall structure are under investigation. Figure 2-2 shows an example of a cross section of the Li target assembly based on the first option. In this option, an yttrium aluminum garnet (YAG) laser will be used to cut the lip seals of the flanges and the target assembly will be moved to the hot cell area for replacement of the back wall itself. The second option is a so-called "Bayonet" type back wall. With this concept the back wall is replaced using a remote handling device, without moving the target assembly. The sliding back wall is mechanically attached to the target assembly. The target assembly is approximately 2.5 m tall, weights about 600 kg, and is supported by arms attached to the sidewall. The vertical test assemblies will be located as close as possible (within about 2 mm) to the target back wall to receive maximum neutron fluence. Nominal vacuum conditions are 10^{-3} Pa in the target chamber and 10^{-1} Pa in the test cell.

2.3 Li main and purification loops

A detail flow diagram of the Li loop including the Li purification loop is shown in

Fig. 2-3. The major components in this loop are the target quench tank, the surge or overflow tank, the Li dump tank, the organic dump tank, the main electromagnetic pump, and two heat exchangers. All of the piping and tanks are constructed of austenitic 316 stainless steel. There are, in addition, a trace heating system (to maintain the temperature throughout the loop above the melting point of the Li at all times the liquid Li is present in the loop), thermal insulation, valves, electromagnetic flow meters, instrumentation, and connections to vacuum and argon headers. The total Li inventory is about 9 m^3. Major impurities in the Li loop are protium, deuterium, tritium, ^7Be, activated corrosion products and other species (C, N, O). Tritium and ^7Be are produced by direct reactions of the deuteron beam with the Li. Deuterium from the beam is also contained in the Li flow. The total estimated production rates of H, D, and T for full power operation are about 5 g/y, 160 g/y, and 7 g/y, respectively. Hydrogen isotopes (H, D, T) are removed by hot trapping with yttrium sponge at 285°C, or, as an option, by the cold trapping with hydrogen sparging. The main highly radioactive impurity will be ^7Be, a 53-d half-life material produced from (d,n) and (d,2n) reactions with Li. The cold trap with 316 SS mesh at 200°C will remove most of the ^7Be, but some is expected to plate out around the loop, and will very likely dominate the remote handling requirements. If not removed, this product will build up to a saturation activity of 4.5×10^{15} Bq (=140 kCi). Activated corrosion products are also highly radioactive impurities. Since remote handling requirement depends on the activation level of the corrosion products, evaluation of corrosion rate and activation levels are urgently needed. Oxygen will also be removed by the cold trap. Nitrogen will be removed by the hot trap at 550°C up to 600°C. Candidate getter materials are V-Ti alloy [2-3], Zr, etc. Nitrogen forms highly corrosive compounds with Li and may build up from air contamination during repair exchange of components and adhesion to component surfaces. Carbon can build up from HX tube leakage. The design value of permissible concentrations of these impurities (C, O, N, H isotopes, and Be) are 10 wppm.

References

[2-1] Nakamura, H., et al., "Latest liquid lithium target design during the key element technology phase in the international fusion materials irradiation facility (IFMIF)", Fusion Eng. and Des. **66-68**, 193(2003).

[2-2] Nakamura, H., et al., "Present status of the liquid lithium target facility in the international fusion materials irradiation facility (IFMIF)", J.Nucl.Maters. **329-333**, 202 (2004).

[2-3] Sakurai,T., et al., "Control of the nitrogen concentration in liquid lithium by the hot trap method", J.Nucl.Maters. **307-311**, 1380 (2002).

Table 2-1. Major design requirements of the IFMIF target system.

Items	Parameters
Deuterium beam energy/current	40 MeV / 125 mA (nominal) x 2 accelerators
Averaged heat flux	1 GW/m^2
Beam deposition area on Li jet	0.2 m^W x 0.05 m^H
Jet width / thickness	0.26 m / 0.025 m
Jet velocity	15 (range 10 ~ 20) m/s
Nozzle geometry	Double-reducer nozzle based on Shima's model
Nozzle contraction ratio	10 (4 : 1st nozzle, 2.5 : 2nd nozzle)
Surface roughness of nozzle	< 6 μm
Curvature of back wall	0.25 m
Wave amplitude of Li-free surface	< 1 mm
Flow rate of Li	130 l/s (at target section)
Inlet Temperature of Li	250°C (nominal)
Vacuum pressure	10^{-3} Pa at Li-free surface 10^{-1} Pa in target/test cell room
Hydrogen isotopes content	< 10 wppm (< 1 wppm T)
Impurity content	<10 wppm (each C,N,O)
Corrosion product content	TBD
Materials (back wall) (other components)	RAF steel or 316 stainless steel 316 stainless steel
Erosion/corrosion thickness (nozzle and back wall) (piping etc.)	 < 1 μm /year < 50 μm /30 years
Replacement	every 11 months for back wall No replacement for 30 years (other components)
Availability	> 95 %

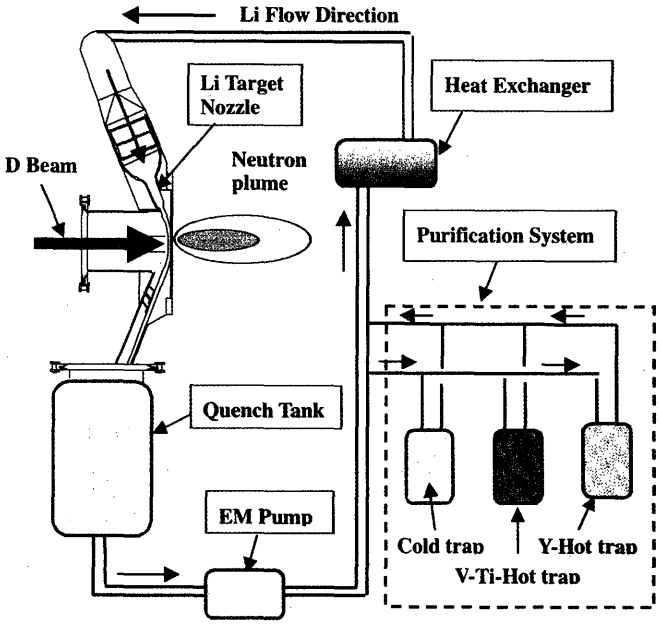

Fig.2-1 Block diagram of the IFMIF Li loop

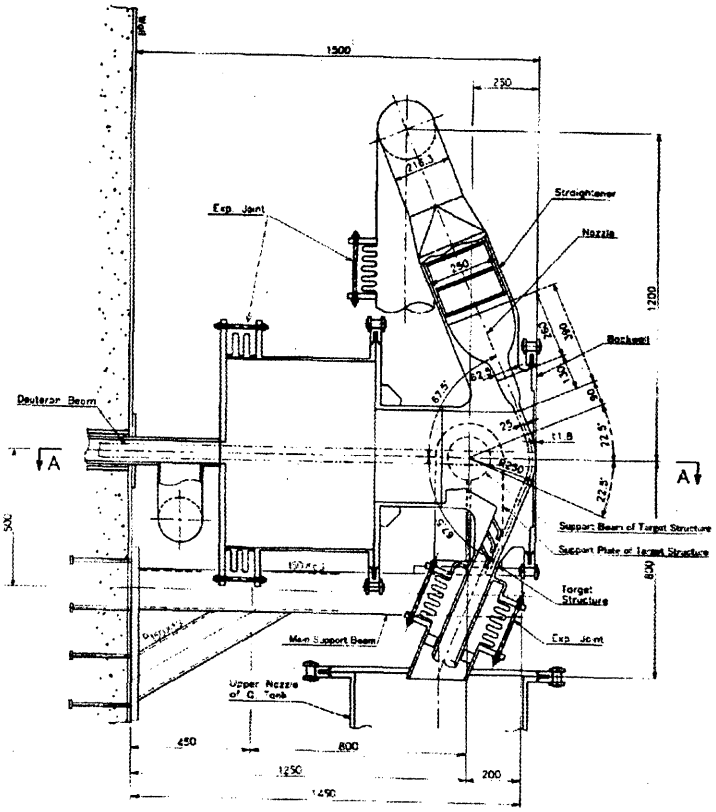

Fig.2-2 Cross section of Target Assembly

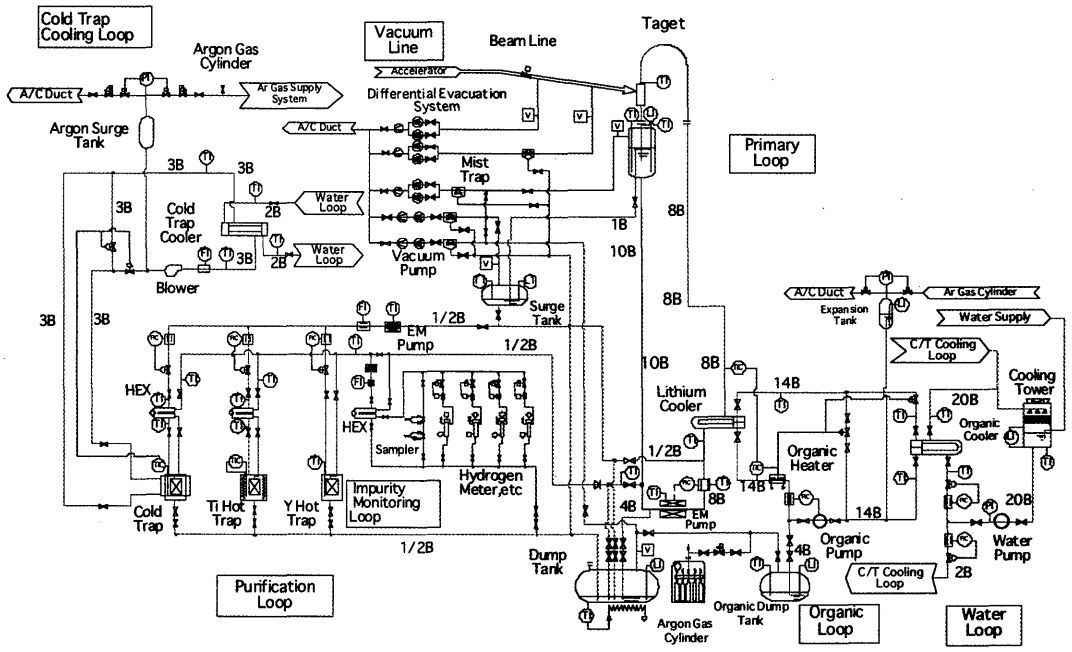

Fig.2-3 Flow Diagram of IFMIF Li Loop

3. Thermal Analysis of Target Assembly

3.1 Thermal condition of target assembly

Thermal condition of the IFMIF target in the test cell is shown in Fig. 3-1. The test cell atmosphere is vacuum (0.1 Pa) condition in operation and 1 atm (~0.1 MPa) Ar in maintenance. Before Li charging and beam operation, a temperature of the target assembly including the backwall should be maintain enough higher than the Li freezing point of 181 °C. Thermal analysis of the target assembly was performed by considering heat balance among heat conduction and radiation. The analysis is divided into two parts. One is that for most of the slant part of the target assembly as shown in Fig. 3-1. Thermal isolation is available for this part. The other is that for a part around the backwall. Thermal isolation is not available for this part because of an installation of the vertical test assembly (VTA) for utilizing neutrons generated by D-Li reaction.

3.2 Analysis for shield and insulation part

3.2.1 Calculation conditions

Calculation model is shown in Fig. 3-2. Two types of thermal isolation shown in also Fig. 3-1 were evaluated in this analysis. One was insulation made of ceramic fiber. The other was thermal shield consisting of SS304 plates with a thickness 0.2 mm and a spacing of 5 mm. Required thickness of these equipment to keep temperatures 300 °C in the target assembly and at about 50 °C outside the equipment was calculated under Ar atmosphere condition of 0.1 MPa and vacuum. Calculation cases are shown in Table 3-1. Typical emissivity: α was assumed 0.2 for the thermal shielding plates, outside of the insulation and wall of the test cell, assuming polished 304 steel. The calculation was performed under such a simplification that the target assembly was a cylinder with a radius of 0.134 m and infinite length. Also the wall of test cell was assumed to be a cylinder with a radius of 1.5 m and a temperature of 20 °C.

3.2.2 Results

As results, required thickness of the thermal shield / insulation was 140, 327, 80 and 75 mm for Cases A1-A4, respectively. Figure 3-3 shows temperature in the thermal shield / insulation. In case of employing the insulation, required thickness is larger than that in case of the thermal shield. In case of vacuum condition, required thickness of the insulation is far larger than that in case of the thermal shielding. Employing the thermal shield is better choice for thermal isolation of the target assembly.

To improve shielding performance of the thermal shield, reducing the emissivity from 0.2 is needed. Figure 3-4 shows required number of the shielding plate as a function of the emissivity. Emissivity, excepting those of the most outside of the shield and wall of the test cell, was changed in this calculation. In Case A3, the number of the plate could not be

reduced to less than 12, since most of heat flux per unit length 120 W/m was made as heat conduction between the shields plates. In Case A4 under vacuum condition, the number of the plate can be reduced to 5 with employing well-polished stainless steel with an assumed emissivity of 0.05 deteriorated from an initial value of 0.02.

3.3 Analysis for non-shield part

3.3.1 Calculation conditions

Calculation model is shown in Fig. 3-5. Thermal shielding is not applicable to a part near the backwall as shown in Fig. 3-1. Only heater is attached to a part around the reducer nozzle. Furthermore, the backwall is located 2 mm (assumed 1.5 mm in the analysis considering an error of 0.5 mm at installation) distant from the VTA with a wall temperature 50 or 150 °C. To prevent Li solidification, Li temperature of 200 °C should be maintained even in case of VTA temperature of 50 °C. Temperature of eleven elements (six for the target assembly, five for the backwall) was calculated considering heat balance among the elements, heaters and VTA. Calculation cases for this non-shield part is shown in Table 3-2. An emissivity of 0.05, 0.1 or 0.2 was assumed for all equipment. A heat transfer between the backwall and the target assembly was 150 or 5000 $W/m^2 \cdot K$. Temperature of 300 °C at the shield part was assumed as a boundary condition.

3.3.2 Results

As results, every minimum temperature was respectively 74, 162, 185, 215, 216, 236, 244, 257, 242 and 256 °C in Cases B1-B10 at center of the backwall, which was most distant from heater and nearest to the VTA. Therefore, the test cell atmosphere should be vacuum condition and the emissivity of the target assembly and VTA should be 0.05-0.1. An effect by heat transfer between the backwall and the target assembly was not significant, since the employed values were enough high in comparison with the heat conduction in the large assembly and the backwall made of stainless steel.

3.4 Required power of the electric heater

Total required capacity of heater was evaluated using the result of Cases A4 with assumption of length of 15 m for the shield part and the result of Cases B3. Heater capacity of 14 kW is sufficient to increase the maximum temperature of the target assembly and pipes from ambient temperature to 300 °C within 5 hours.

3.5 Summary

The thermal analysis of the target assembly is summarized as follows:

1) Thickness of the thermal shield can be reduced to 20 mm by employing stainless steel with

emissivity of 0.05.

2) Liquid Li should be charged and circulated under vacuum condition and the emissivity of the target assembly and VTA should be 0.05-0.1.
3) Total required capacity of the heater system would be 14 kW.

In a case of 0.1 Pa in the test cell, structural design of the test cell room is not easy. Therefore, to mitigate structural design of the test cell room, operation under 0.1 MPa He is proposed. At present, design option of the target assembly compatible with He environment slightly less than 0.1 MPa is being in progress. In this case, electric heater is needed on the backwall outer surface to maintain temperature of the backwall during start-up phase.

Table 3-1 Calculation cases and results for thermal shielding / insulation.

Case	Input conditions		Results	
	Thermal isolation	Test Cell atmosphere	Required thickness (mm)	Heat flux per unit length (W/m)
A1	Insulation	0.1MPa Ar	140	165
A2	Insulation	Vacuum	327	94
A3	Shielding	0.1MPa Ar	80 (17 Layears)	130
A4	Shielding	Vacuum	75 (16 Layears)	46

Table 3-2 Calculation cases and results for non- shield part of target assembly.

Case	Input conditions				Results	
	Test Cell atmosphere	VTA temp. (°C)	Emissivity	Heat transfer ($W/m^2 \cdot K$)	Minimum temp. (°C)	Heat loss (W)
B1	0.1MPa Ar	50	0.2	5000	73.8	180
B2	0.1MPa Ar	150	0.2	5000	161.5	133
B3	Vacuum	50	0.2	5000	185.1	149
B4	Vacuum	150	0.2	5000	214.8	116
B5	Vacuum	50	0.1	5000	216.1	79
B6	Vacuum	150	0.1	5000	236.3	61
B7	Vacuum	50	0.05	5000	243.6	43
B8	Vacuum	150	0.05	5000	256.5	33
B9	Vacuum	50	0.05	150	242.3	43
B10	Vacuum	150	0.05	150	255.6	33

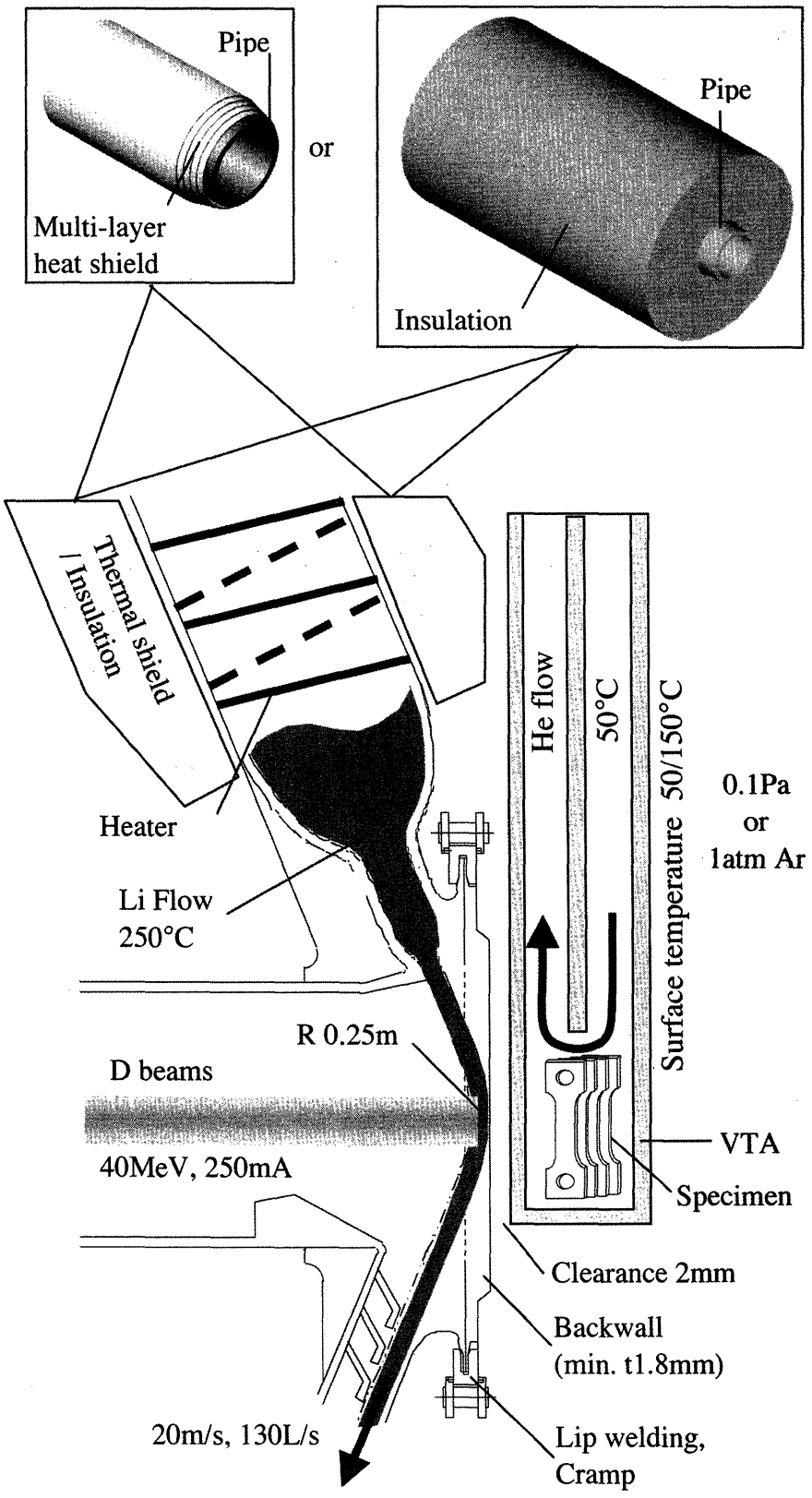

Fig. 3-1 Cross-sectional view of beam-target interaction and VTA.

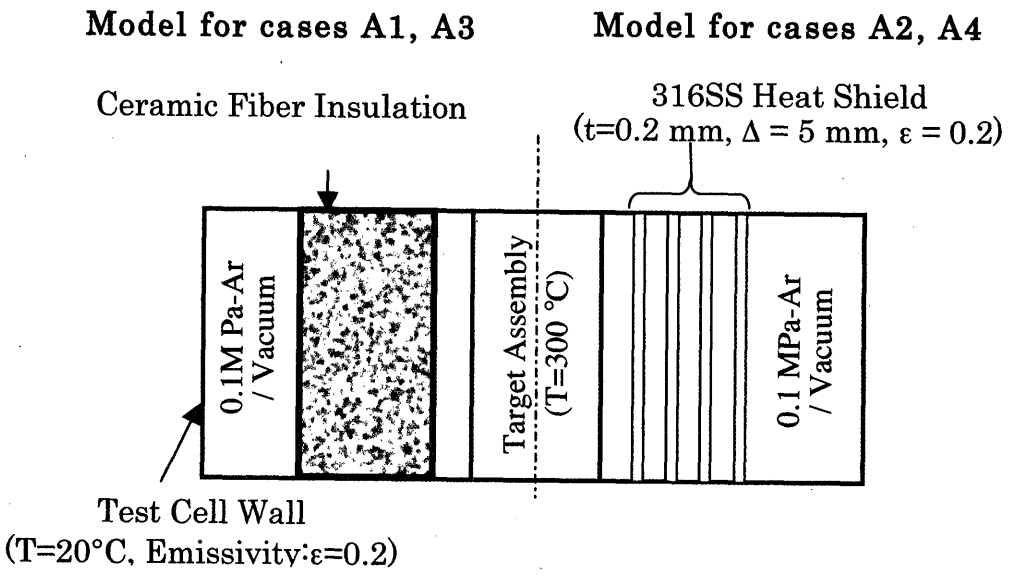

Fig. 3-2 1-D cylindrical calculation models for Cases A1,A3 and A2,A4.

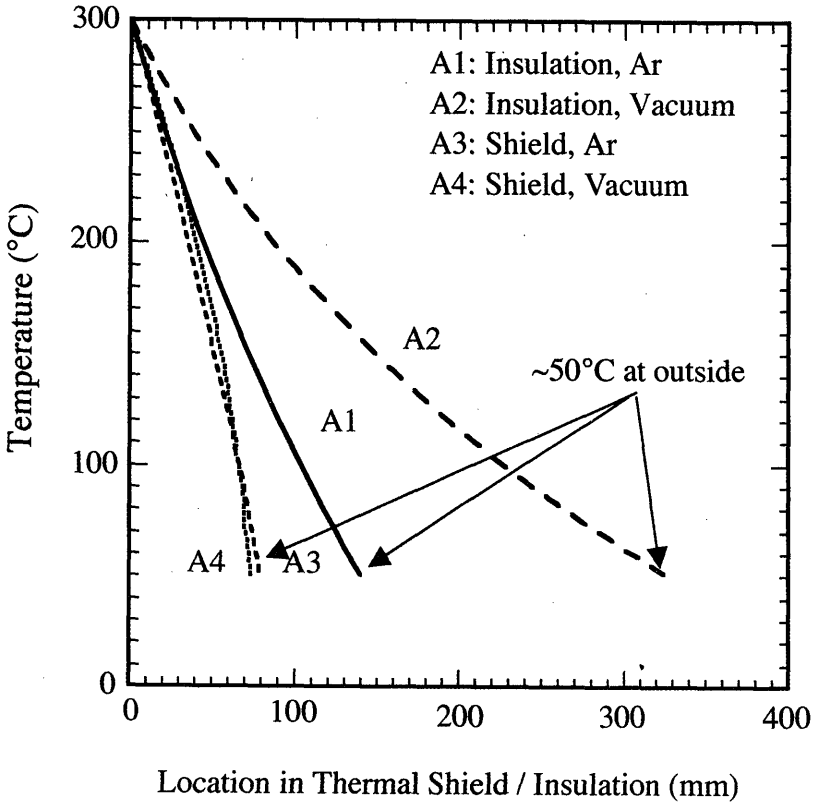

Fig. 3-3 Temperature in thermal shield/ insulation.

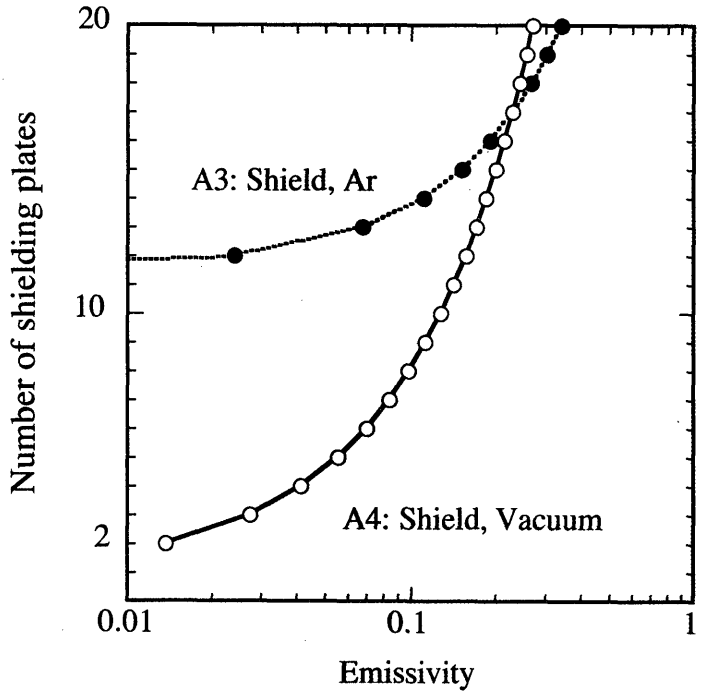

Fig. 3-4 Required number of shielding plates depending on emissivity.

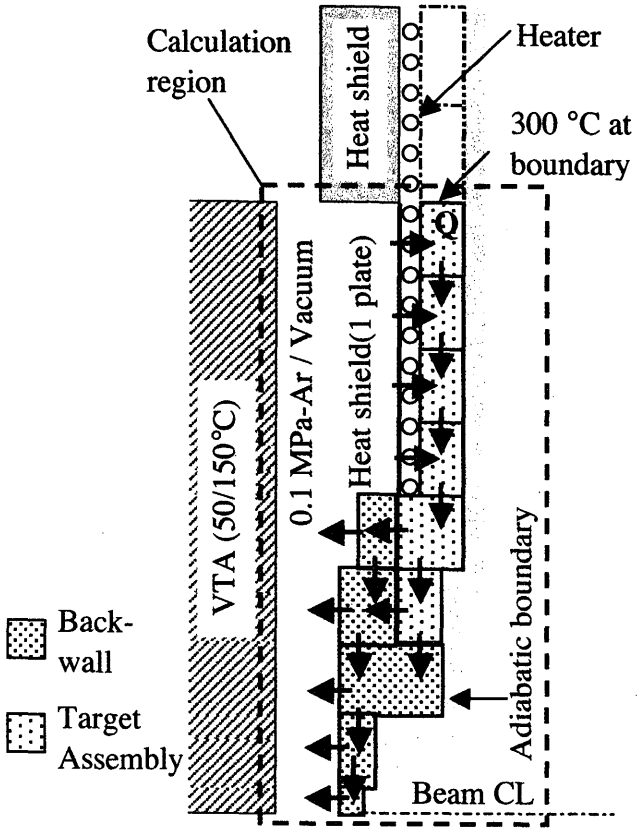

Fig. 3-5 Calculation model for Cases B1-B10.

4. Thermo-mechanical Analysis of Back Wall

4.1 Calculation model

A backwall attached to an IFMIF target assembly suffers most intense neutron irradiation equivalent to about 50 dpa a year among IFMIF equipment. Deformation of the backwall due to temperature distribution under condition of neutron irradiation was estimated by using an FEM code ABAQUS Ver 6.3.1[4-1]. Figure 4-1 shows three-dimensional view of the backwall. Its shape is nearly a disc with a diameter of 715 mm. Its Li-side has a concave face with radius of 250 mm, which is wetted by liquid Li. The Li-side has also a flat face (X = 0 mm), which is contacted to a target assembly. The minimum thickness 1.8 mm of the backwall is given at its center (Y = 0 mm, Z = 0 mm). As shown in Fig. 3-1, the backwall is connected to the target assembly by welded lip seal and mechanical cramp at the circumference. Both parts are assumed made of 316 stainless steel in this calculation.

4.2 Calculation condition

Figure 4-2 shows nuclear heat by neutron irradiation [4-2]. The maximum value 25 W/cm^3 was given at a beam center (Y = 0 mm, Z = 0 mm), where the wall thickness was 1.8 mm. The analysis was performed for a 1/4 section (0 mm < Y, 0 mm < Z) of the backwall because of its symmetry. This 1/4 section consists of 35,170 elements and 40,338 nodes as shown in Fig. 4-3. Heat transfer between the backwall and the target assembly: α was 15.8 or 150 W/m^2·K depending on contact pressure due to clamping, which was assumed 0.1 or 1.0 MPa. Deformation of the backwall depends on also constraint conditions at its circumference. Two cases for the constraint condition were considered at the circumference of the disc. One is a constraint for all degrees of freedom, and the other is that only in X direction. The analysis cases are summarized in Table 4-1. Temperatures of the target assembly and liquid Li were both 300 °C, and heat transfer coefficient between Li and 316 steel was 34 kW/m^2·K. Pressure in a test cell room, where the backwall and the target assembly were installed, was assumed vacuum. An emissivity of stainless steel 316 was 0.3.

4.3 Results

Backwall temperature is shown in Figs. 4-4 and 4-5. Even with nuclear heating by the neutrons, temperature of the concave part is about 300 °C due to cooling by Li flow. In Cases C1 and C3, the maximum temperature was 440 °C. In Cases 2 and 4, the temperature distribution was nearly equal to that in Cases C1 and C3. The maximum temperature was 445 °C. Effect of VTA temperature: T_{VTA} upon the backwall temperature was found to be negligible.

Figures 4-6 through 4-9 show calculated stress in Cases C1 through C4. Case C-3 gives the minimum stress among Cases C1-C4 with a heat transfer coefficient of 15.8 W/m^2·K. Even in

this case, thermal stress was about 500 MPa at the concave part.

Figures 4-10 and 4-11 show calculated displacement in Cases C2 and C4. The displacement significantly depends on the constraint condition. The displacement of +5.2 mm in X-direction in Case C-2 exceeded a designed clearance of 2.0±0.5 mm between the target assembly and VTA. Even in Case C-2, displacement of the backwall center was –2 mm in X-direction. This local displacement made convex part on the concave surface, and would consequently make instability on the high-speed free-surface flow of the Li target.

However, in Cases C5 and C6 with increased heat transfer coefficient of 150 $W/m^2 \cdot K$, the maximum temperature was about 380 °C as shown in Fig. 4-12. Thermal stress was reduced to about 260 MPa and the backwall displacement became -0.3 mm in X-direction, as respectively shown in Figs. 4-13 and 4-14. To reduce the stress and deformation in the IFMIF backwall, a high heat transfer coefficient of more than 150 $W/m^2 \cdot K$ in the contact surface will be required and the structural design of the backwall and the target assembly will proceed in the next design stage.

4.4 Summary

The thermal-stress analysis are summarized as follows:

1) The backwall deformation would be reduced from 2 to 0.3 mm by increasing heat transfer coefficient from 15.8 to 150 $W/m^2 \cdot K$.

References

[4-1] Hibbitt, Karlsson & Sorensen, Inc., ABAQUS User's Manual.

[4-2] Gomes, I. C. , "Nutronics Analysis, in IFMIF-CDA Team (ed. H. Maekawa and S. Konishi), Minutes of the Second IFMIF-CDA Design Integration Workshop May 20-25, 1996, JAERI, Tokai, Japan", JAERI Report, JAERI-Conf 96-012, 1996, pp.288-290.

Table 4-1 Calculation cases and results of thermo-mechanical analysis.

Case	Input conditions			Results				
	Heat transfer ($W/m^2 \cdot K$)	Direction of constraint	VTA temp. (°C)	Max. temp. (°C)	Max. stress (MPa)	Max. displacement (mm)		
						X	Y	Z
C1	15.8	X, Y, Z	50	440.2	1003	+4.9	+0.54	+0.54
C2	15.8	X, Y, Z	150	444.5	1065	+5.2	+0.57	+0.56
C3	15.8	X	50	440.2	485.5	-2.0	+0.63	+0.72
C4	15.8	X	150	444.5	504.7	-2.2	+0.67	+0.76
C5	150.0	X	50	379.5	261.5	-0.29	+0.24	+0.26
C6	150.0	X	150	381.1	266.8	-0.33	+0.25	+0.27

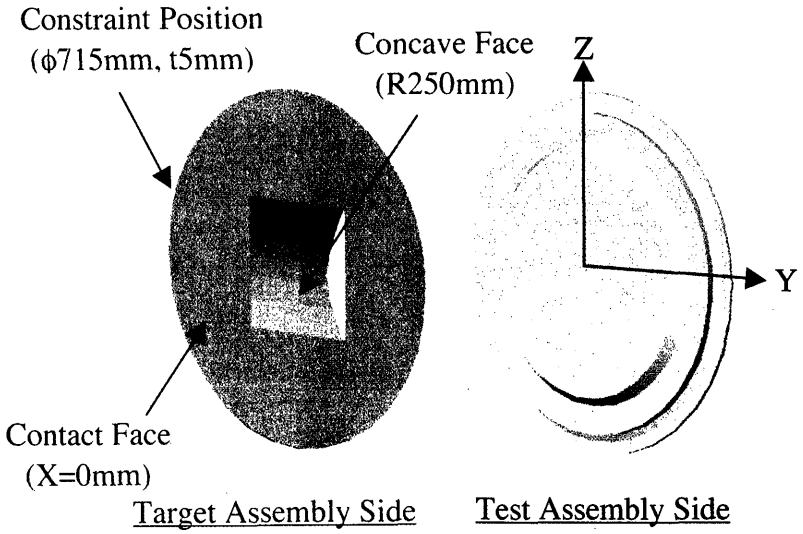

Fig. 4-1 IFMIF target backwall.

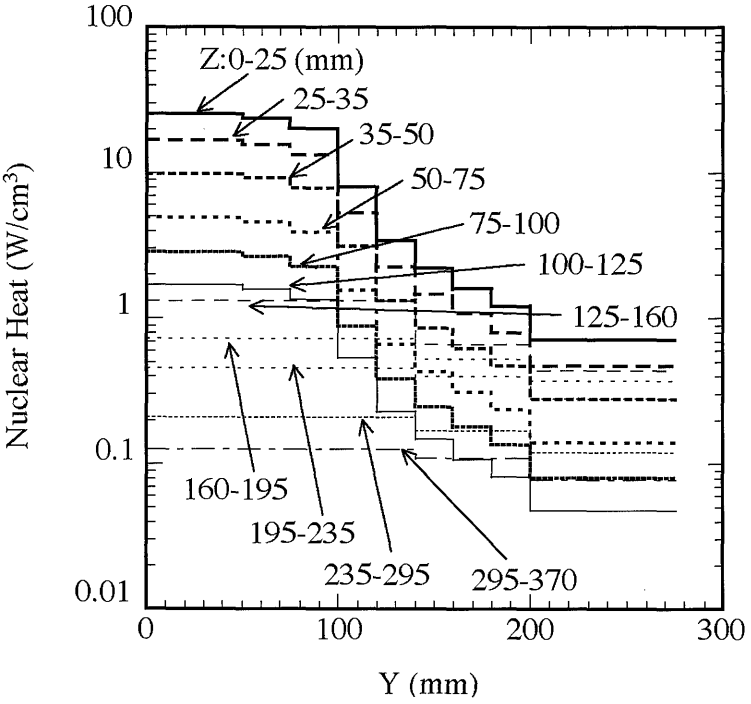

Fig. 4-2 Nuclear heat in Backwall.

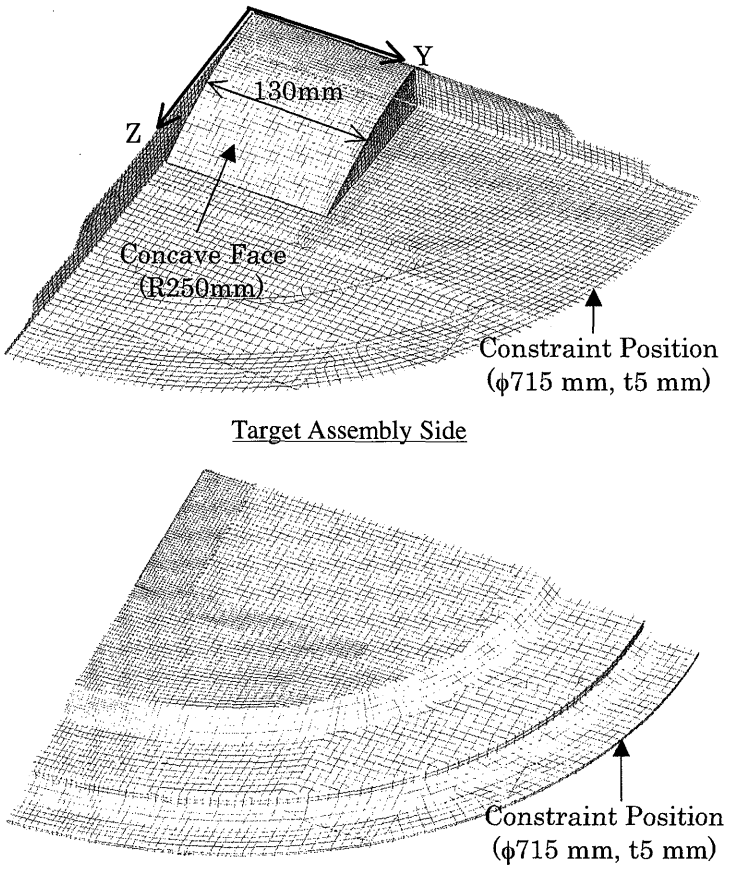

Fig. 4-3 Calculation model of backwall.

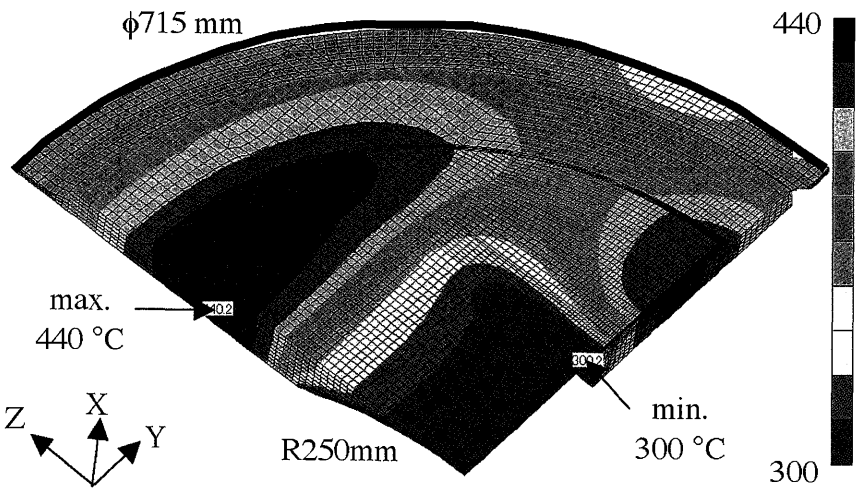

Fig. 4-4 Temperature in Cases C1, C3
(T_{VTA} = 50 °C)

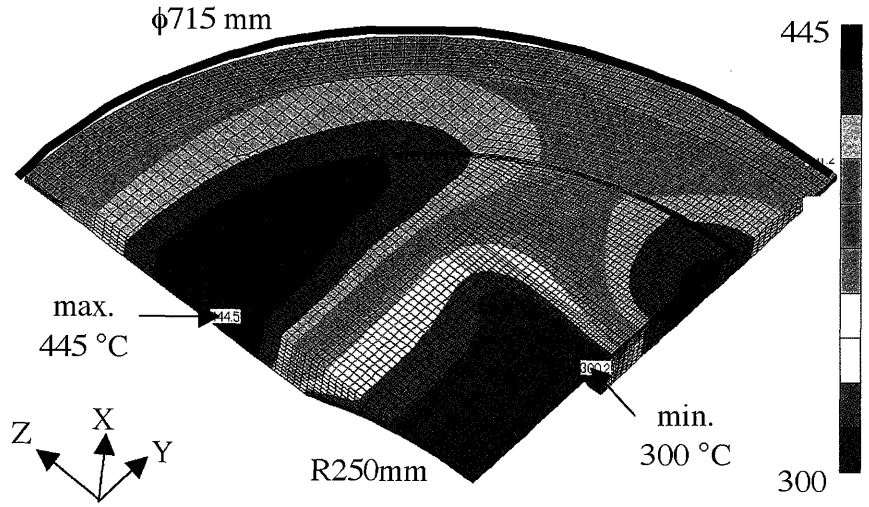

Fig. 4-5 Temperature in Cases C2, C4
(T_{VTA} = 150 °C)

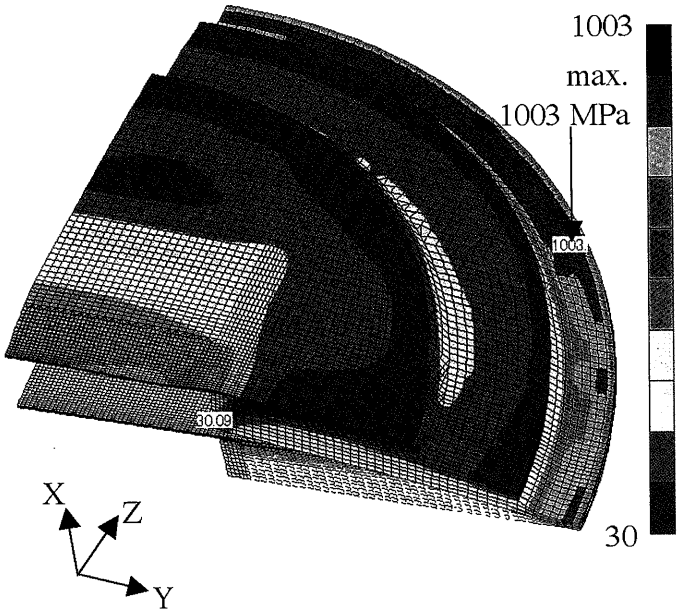

Fig. 4-6 Stress in Case C1
(Fully rigid, T_{VTA} = 50 °C)

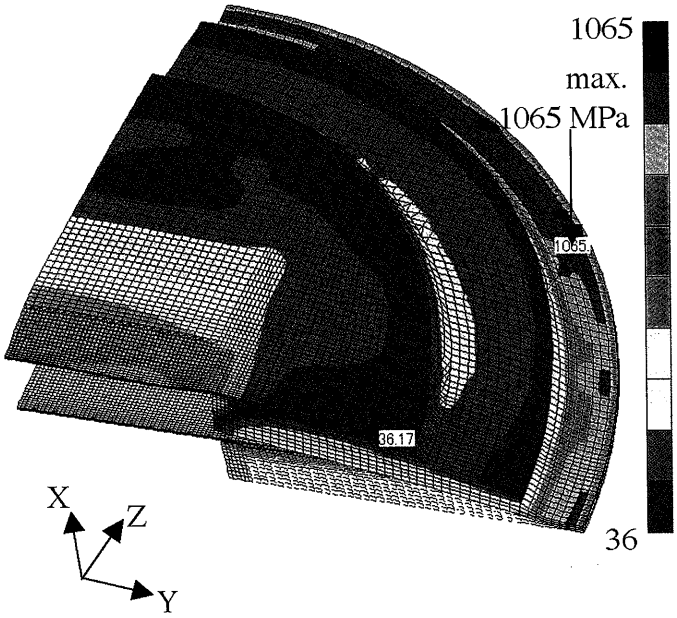

Fig. 4-7 Stress in Case C2
(Fully rigid, T_{VTA} = 150 °C)

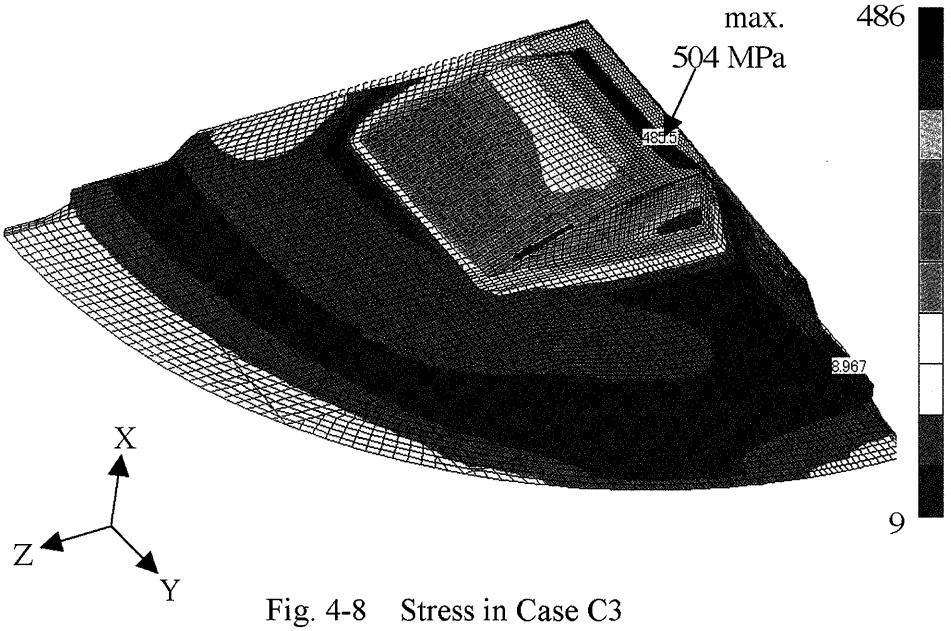

Fig. 4-8 Stress in Case C3
(Free in Y, Z directions, T_{VTA} = 50 °C)

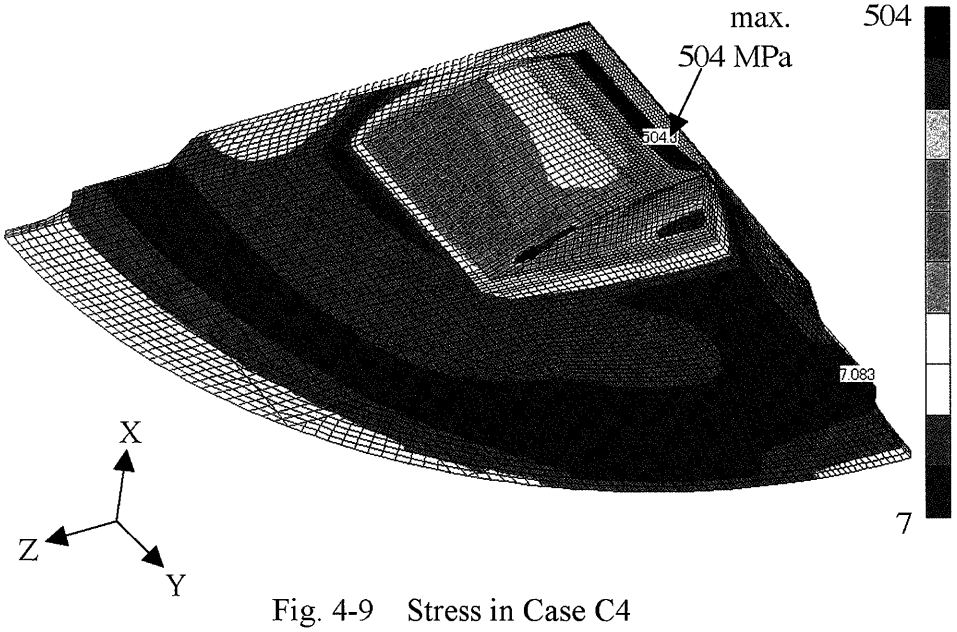

Fig. 4-9 Stress in Case C4
(Free in Y, Z directions, T_{VTA} = 150 °C)

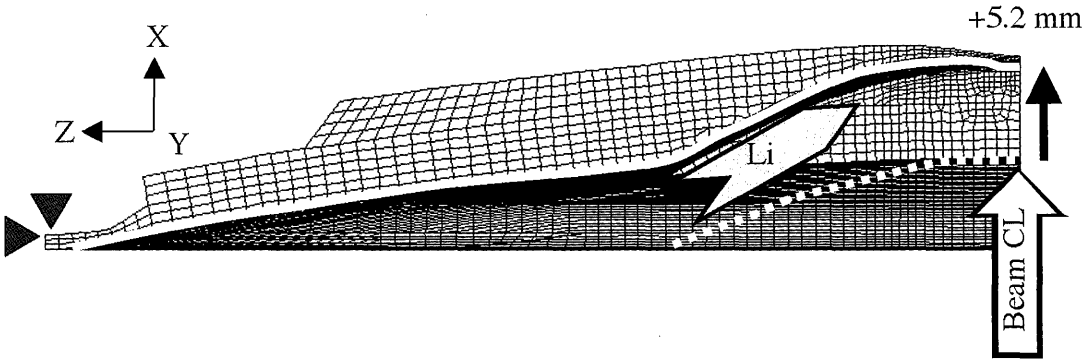

Fig. 4-10 Displacement in Case C2
(Fully rigid, T_{VTA} = 150 °C)

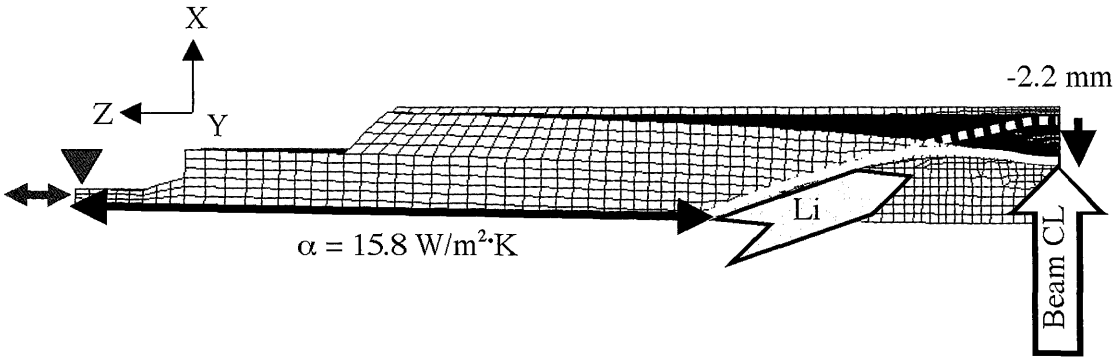

Fig. 4-11 Displacement in Case C4
(Free in Y, Z directions, T_{VTA} = 150 °C)

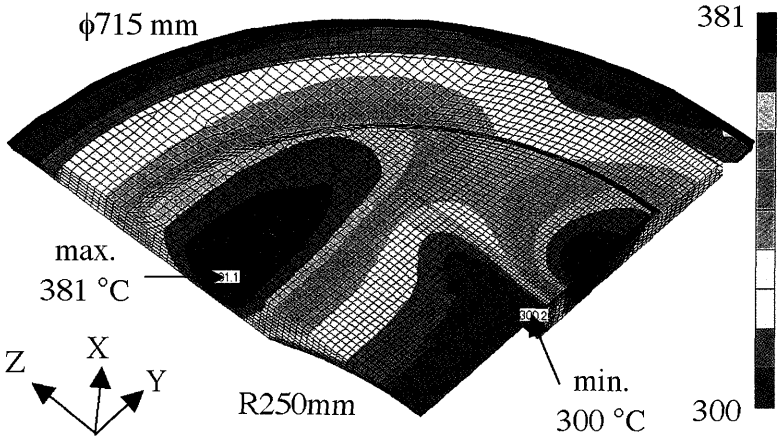

Fig. 4-12 Temperature in Case C6
(Free in Y, Z directions, α = 150W/m^2·K, T_{VTA} = 150 °C)

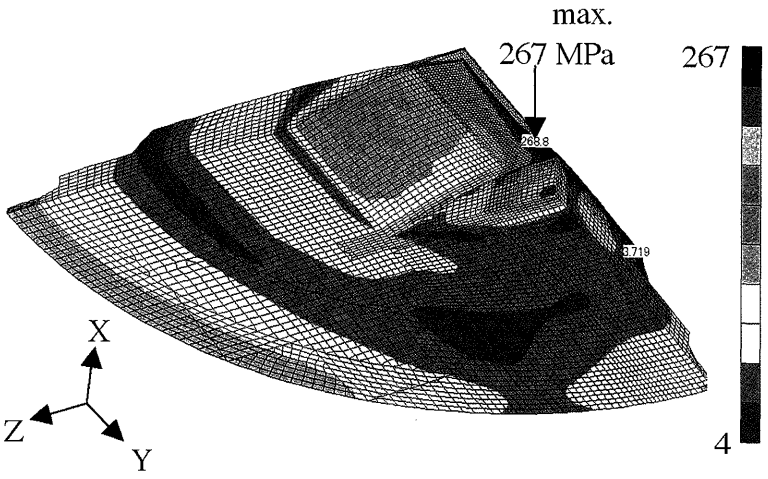

Fig. 4-13 Streaae in Case C6
(Free in Y, Z directions, α = 150W/m^2·K, T_{VTA} = 150 °C)

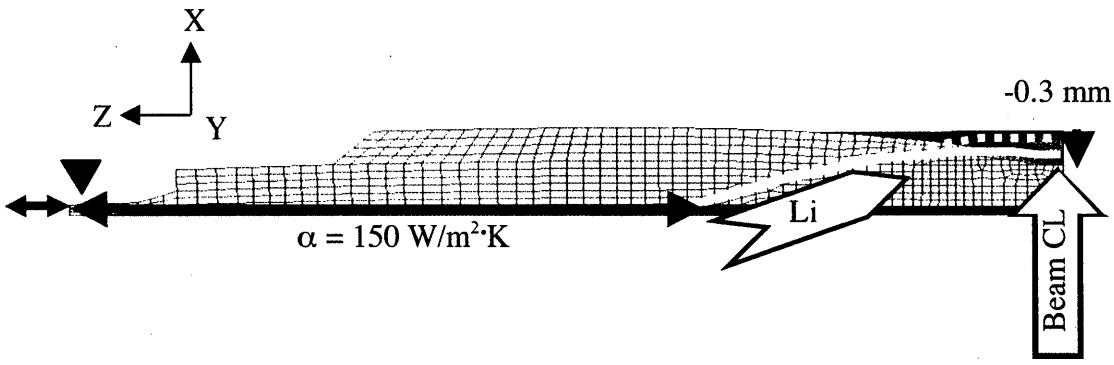

Fig. 4-14 Displacement in Case C6
(Free in Y, Z directions, α = 150W/m·K, T_{VTA} = 150 °C)

5. Radiation Dose Rate around the Li Loop Components

5.1 Introduction

Neutrons are produced in the Li flow and emitted through a back wall to high flux test module. Since the back wall will be activated under intense irradiation of about 50 dpa/year, replacement of Li target assembly including the back wall is performed by a remote handling system. However, activated materials of the back wall are transferred into the Li flow due to erosion/corrosion process and deposit on inner surface of the Li loop components. Therefore, accessibility around the Li loop piping will depend on a radiation dose rate caused by the deposition of the activated materials. In this section, the accessibility evaluation of the IFMIF Li loop is described considering the deposition of the activated corrosion products.

5.2 Activation Calculation

The flow of calculation procedure is shown in Fig.5-1. Main process comprises calculations of the neutron spectrum on the target back wall and radioactivity in the wall on the basis of the spectrum. Prior to the calculation of the radioactivity, an activation cross section library was preliminarily compiled for the present analysis. Activation level of the back wall is calculated by the ACT-4 of the THIDA-2 system [5-1] developed in JAERI for activation evaluation of a fusion reactor. The neutron flux spectra at the IFMIF target back wall calculated with McDeLicious code [5-2] is shown in Fig.5-2. Highest energy in these spectra is 56 MeV. But, the existing cross section library for the ACT-4 code has a maximum energy of 15 MeV and an energy structure of 42 groups. Therefore, the cross section of the IEAF-2001 [5-3] with an energy range up to 150 MeV was employed for the activation calculation above 15 MeV. The highest energy group (13.72 MeV – 56 MeV) of the ACT-4 has been replaced by the effective cross section evaluated using IEAF-2001 in the energy range between 15 MeV and 56 MeV. Activation calculations are performed for the back wall with a composition of stainless steel 316LN [5-4] although low activation Ferritic/Martensitic steel is also one of candidate materials. One year full power operation of IFMIF with a deuterium beam current of 250 mA is assumed.

5.3 Back Wall Activation

As a function of the cooling time up to one year, the total and specific activities of the

back wall calculated by the ACT-4 are shown in Fig.5-3. Total radioactivity one hour after the shut down is $4.0x10^{14}$ Bq/kg. The total radioactivity gradually decreases up to one year after the shut down. The total activities after 1 day, 1 week, 1 month and 1 year cooling are $3.1x10^{14}$, $2.8x10^{14}$, $2.3x10^{14}$ and $7.5x10^{13}$ Bq/kg, respectively. Just after shut down, Co-58 with a half-life of 2.33 month is dominant in the total activity up to 3 month. Up to 3 month after the shut down, the other dominant species with a activity more than 10^{13} Bq/kg are Co-56, Mn-54 and Co-57.

5.4 Accessibility Evaluation

Using the total specific activities after one year IFMIF operation calculated by the ACT-4 code, radiation dose rate around the Li loop piping is calculated by QAD-CGGP2R code [5-5]. In the accessibility evaluation, the radioactive corrosion product is supposed to be generated in a beam foot print 100 cm^2 in area. The corrosion rate is selected as 1 μm/y using the data from FMIT project [5-6]. Composition of the corrosion product in Li flow is assumed to be same as stainless steel 316LN. Measurements of the corrosion product composition are performed in ENEA and IPPE. The radioactive corrosion products from the back wall area are deposited in a Li loop components with a total surface area of 572 m^2 where the largest surface area is 532 m^2 in the Li heat exchanger. In the IFMIF Li purification system, a cold trap removes the corrosion products. Although at present quantitative efficiency of the cold trap is not available, the efficiency more than 90% is expected. As a reference case, the radiation dose rate around the piping near an electromagnetic pump is calculated. Inner and outer diameters of the pipe are 248.8 mm and 267.4 mm, respectively. Figure 5-3 shows the dose rate around the piping in a case of 100% deposition (100% plate-out) of the corrosion materials and uniform deposition on inner surface of Li loop piping. Figure 5-4 shows the dose rate as a function of the days after the shut down. Permissible level for hands-on maintenance is selected as 10 μSv/hr. As the results, in the case of 100% plate-out hands-on maintenance is not permitted until one year cooling down. However, in the case of 10% deposition of the corrosion materials (10% plate-out), hands-on maintenance becomes possible. Therefore, reliable operation of the cold trap with a removal rate more than 90 % is needed. During the engineering validation and engineering design activity phase planned in the IFMIF project, performance of the Li purification system including the cold trap will be validated [5-7]. In future, radiation

dose rates around the cold trap, the hot trap and the Li heat exchanger will be evaluated.

In addition, according to preliminary analysis of the radioactivity by ^{7}Be with a half-life of 53 days, the surface dose rate of the Li pipings after 1 month from the shut-down is in a range of 10^{5} μSv/hr in a case of 100% deposition. Therefore, further studies including characteristics of ^{7}Be removal and remote maintenance are necessary to establish reliable design of the Li loop.

5.5 Summary

Activation level of the back wall is calculated by the ACT-4 code of the THIDA-2 system. The activities after 1 day, 1 week, 1 month and 1 year cooling are 3.1×10^{14}, 2.8×10^{14}, 2.3×10^{14} and 7.5×10^{13} Bq/kg, respectively. After a shut-down, Co-58 with a half-life of 2.33 month is dominant in the total activity for 3 months. After that, Mn-54 and Co-57 become dominant in the total activity. Radiation dose rate around the Li loop pipe near the electromagnetic pump is calculated by QAD-CGGP2R code. In the case of 10% deposition of the corrosion materials (10% plate-out), hands-on maintenance becomes possible assuming a permissible level of 10 μSv/hr. Therefore, a removal of radioactive material in Li more than 90 % is needed for the maintenance work. Also, further study on ^{7}Be control is needed.

References

[5-1] Seki, Y., et al., JAERI-Report, JAERI-1301 (1985)

[5-2] Fisher, U., Simakov, S.P. and Wilson, P.P.H., "Transmutation behavior of Eurofer under irradiation in the IFMIF test facility and fusion power reactors", J.Nucl.Maters. **329-333,** 228 (2004).

[5-3] Korovin, Yu. et al., in : International Conference on Nuclear Data for Science and Technology(*ND2001*),7-12 October, 2001,Tsukuba, Japan.

[5-4] ITER Nuclear Analysis Report, G73 DDD 2 01-06-06 W0.1

[5-5] Sakamoto, Y. and Tanaka, S., JAERI-Report, JAERI-M 90-110 (1990).

[5-6] Chopra, O.K. and Tortorelli, P.F., "Compatibility of materials for use in liquid-metal blankets of fusion reactors", J.Nucl.Maters. **122&123,** 1201(1984) .

[5-7] Nakamura, H., Riccardi, B., Loginov, N., Ara, K., Burgazzi, L., et al., "Present Status of the liquid lithium target facility in the international fusion materials irradiation facility (IFMIF) ", J.Nucl.Maters. **329-333,** 202 (2004).

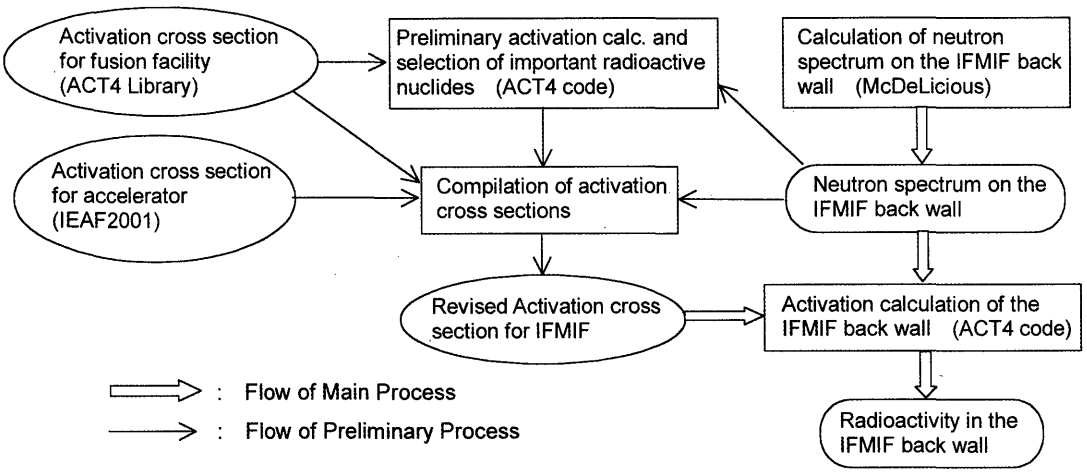

Fig.5-1 Flow diagram of the calculations for the IFMIF back wall activation.

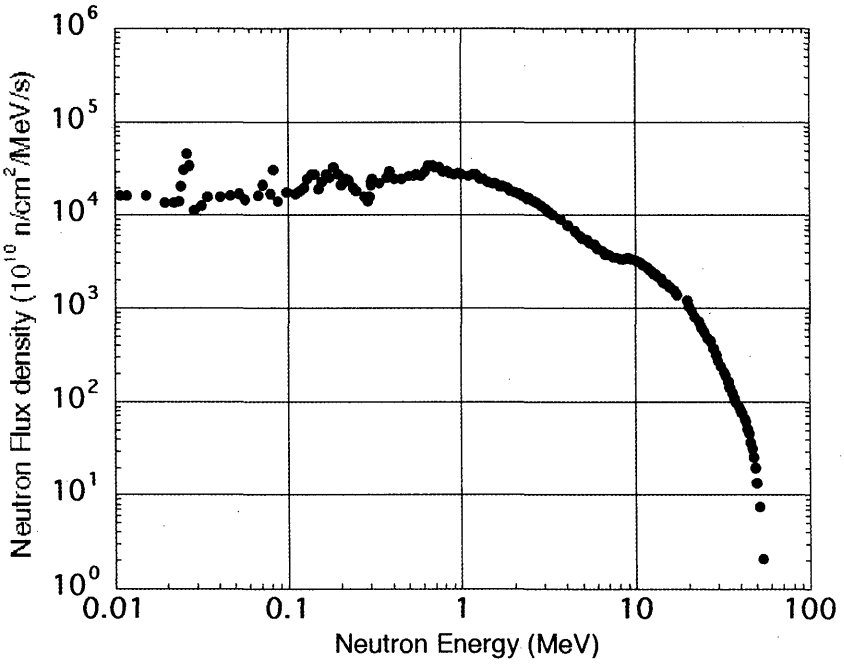

Fig.5-2 Neutron flux density at the IFMIF back wall as a function of neutron energy

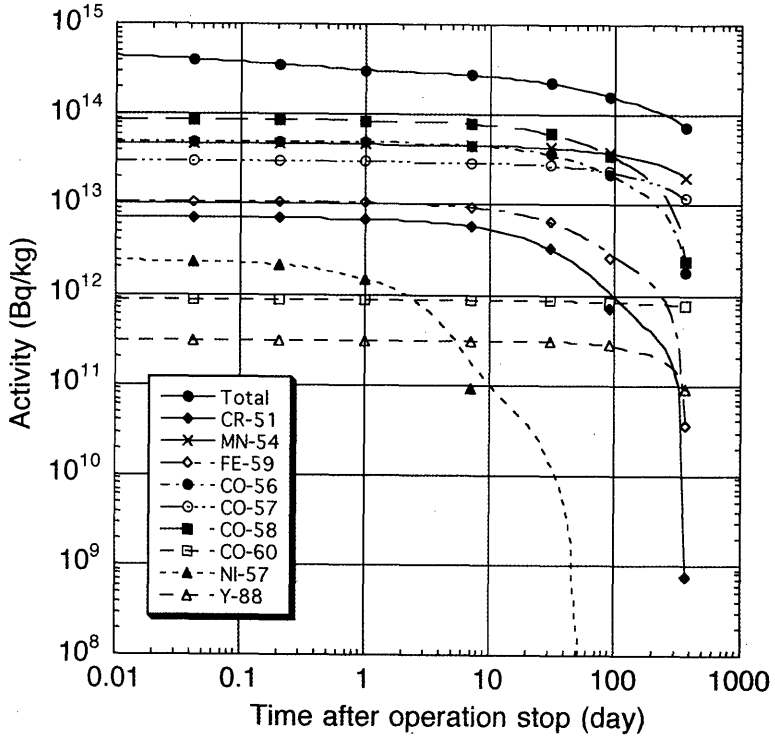

Fig.5-3 Decay of radioactivities of main radioisotopes in the back wall.

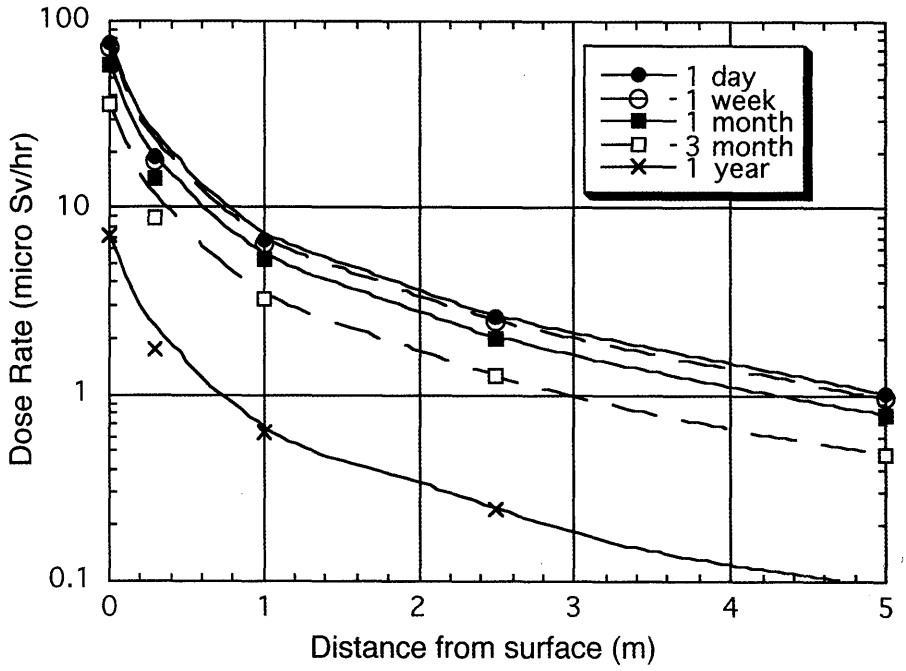

Fig.5-4 Dose rate around the IFMIF Li loop as a function of distance from the surface with a plate-out ratio of 100 %.

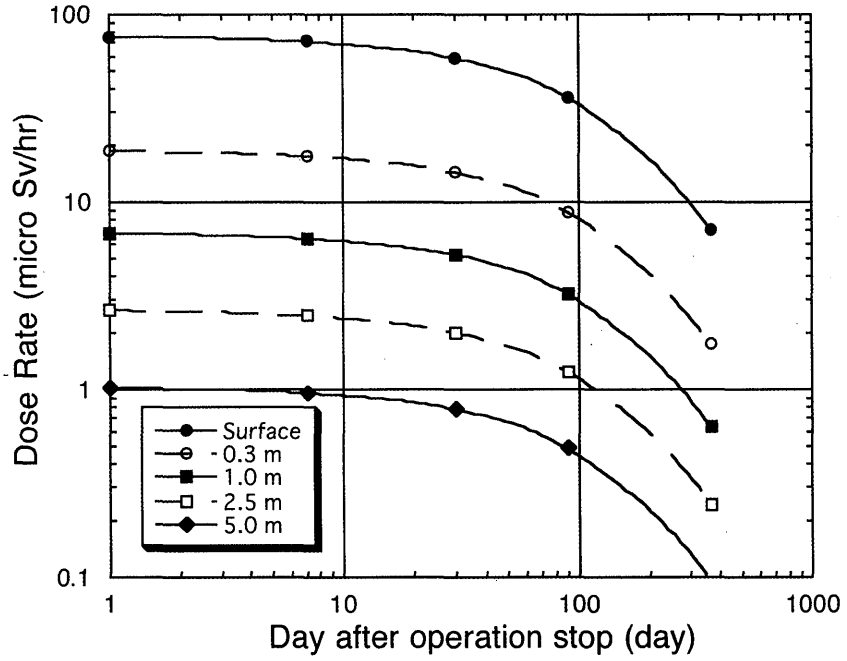

Fig.5-5 Dose rate around the IFMIF Li loop as a function day after operation stop with a plate-out ratio of 100 %.

6. Tritium Inventory of Lithium Loop

6.1 Introduction

In the IFMIF, tritium is produced by D-Li stripping reaction between 40 MeV deuterium and liquid Li. Most of the generated tritium is removed by an yttrium hot trap in the Li purification loop, where impurities in the liquid Li are removed. However, a part of the tritium remains in the Li loop, and permeates through the wall of the Li loop components. The permeated tritium is released to the Li loop area filled with Ar gas or to test cell area. It is important for the safety of the IFMIF to evaluate the amount of tritium permeation and inventory in the Li loop of the IFMIF target system. In this section, the tritium inventory and permeation of the IFMIF Li loop are evaluated.

6.2 Li Target and Tritium Generation

Figure 6-1 shows the block diagram of the IFMIF lithium target system. Main loop to provide a stable Li jet consists of target, a quench tank, an electromagnetic pump, a heat exchanger and pipes between them. Purification loop to remove the impurities in Li consists of a V-Ti hot trap for nitrogen [6-1], an yttrium hot trap for tritium and a cold trap for C, O and ^{7}Be.

In the Li loop, tritium is typically produced by following reactions.

$$D+{}^{7}Li \rightarrow T+{}^{6}Li \quad (6\text{-}1)$$

$$n+{}^{6}Li \rightarrow T+He \quad (6\text{-}2)$$

Tritium is also produced by following reactions.

$$D+{}^{7}Li \rightarrow D+T+{}^{4}He \quad (6\text{-}3)$$

$$D+{}^{7}Li \rightarrow p+D+2T \quad (6\text{-}4)$$

$$D+{}^{7}Li \rightarrow 2T+{}^{3}He \quad (6\text{-}5)$$

$$n+{}^{7}Li \rightarrow n+T+{}^{4}He \quad (6\text{-}6)$$

The amount of generated tritium in the IFMIF is 3.0×10^{11} Bq/h [6-2]. The tritium is removed by absorbing to yttrium getter in the yttrium hot trap. Hydrogen can be absorbed up to a saturation concentration. Beyond the saturation concentration, yttrium hydride will be deposited in the liquid Li. At 558 K of the operational temperature of

the yttrium hot trap, hydrogen concentration should be lower than 24 appm (0.66 appm for tritium). In the calculation, the tritium concentration is assumed to be 0.66 appm for the present estimation.

6.3 Calculation

The tritium in the liquid Li adheres to the inner surface of the components in accordance with the distribution coefficient between liquid Li and wall material. Then the tritium diffuses in the wall, and leaks out. The tritium concentration C_s of the inner surface is given by

$$C_s = C_{Li} \times K_d \tag{6-7}$$

where C_{Li} is the tritium concentration in liquid Li and K_d is the distribution coefficient. The distribution coefficient between liquid Li and 316 stainless steel as a reference wall material of the IFMIF Li loop is not known at this stage. Therefore, the estimated value for 18Cr-8Ni steel (304 stainless steel) is used as follows [6-3].

$$\ln K_d = 2.52 - 7500/T \tag{6-8}$$

where T is temperature (K).

In this paper, the tritium permeation and inventory in steady state are calculated for conservative evaluation, because they give maximum value. And the hydrogen concentrations are steady state at surface attached Li and the surface of backside is zero. The permeation rate through unit area of a plane in steady state is given by

$$J = D\frac{C_s}{d} \tag{6-9}$$

where J is the permeation rate, D is the diffusion coefficient, and d is the thickness of a plane. The diffusion coefficient in 316 stainless steel is used as follows [6-4].

$$D = 6.32 \times 10^{-7} \exp(-5750/T) \tag{6-10}$$

The permeation rate through unit length of a pipe in steady state is given by below equation [6-5].

$$J = 2\pi D \frac{C_s}{\ln(1 + d/a)} \tag{6-11}$$

where a is the inner radius of a pipe, and d is the thickness of a pipe.

On the other hand, the tritium contained in the Li loop components is evaluated by steady state tritium depth profile in the wall. The regions evaluated the tritium permeation rate and inventory are the main loop components (the target, the quench tank, the heat exchanger and pipes), the pipes between main and purification loops, the V-Ti hot trap (873 K), the yttrium hot trap (558 K) and the cold trap (473 K). These specifications are shown in Table 6-1.

6.4 Results and Discussion

The tritium permeation rates through the wall wet by the Li loop of the IFMIF are shown in Fig. 6-2. The amount of total tritium permeation rate is 1.0×10^{6} Bq/h. Which is much smaller than the generated tritium (3×10^{11} Bq/h) in the Li flow. Therefore, most of the generated tritium deposits to the liquid Li or to the Y hot trap. About 95 % of the tritium permeation from the Li loop components is one at the V-Ti hot trap. This reason is that the product of the diffusion and distribution coefficients at 873 K of the operating temperature of the V-Ti hot trap is 4 orders of magnitude greater than one at 523 – 558 K of the operating temperature of the other regions. In the main loop components, the tritium permeation rate through the heat exchanger is most large, because the surface area of the pipes for heat transfer is about 444 m^2, which is larger than total surface area of the other Li loop components. The tritium permeated through the pipes for the heat transfer solves to organic oil. Then the tritium in the organic oil release to the Li loop area, or solves to water at a heat exchanger for the organic oil. In this section, it is assumed that the permeated tritium from the heat exchanger release to the Li loop area.

Figure 6-3 shows the flow chart of the tritium processing for permeated tritium from the liquid Li. The value at each area is the generated rate of tritium, and the values at each detritiation system are maximum tritium concentration which can be processed by the detritiation system and maximum achieved tritium concentration. The permeated

tritium from the target, the quench tank, and a part of the pipe in the main loop releases to the test cell. Tritium contaminated vacuum exhaust from the test cell is processed by the exhaust detritiation system for tritium contaminated air. The tritium permeation rate from the Li loop to the test cell is 5×10^{2} Bq/h, and the tritium concentration of the vacuum exhaust is 5×10^{-2} Bq/cc, which can be processed by the exhaust detritiation system for tritium contaminated air.

The permeated tritium from the other components of the IFMIF Li loop releases to the Li loop area. The Li loop area is filled with Ar gas to eliminate the possibility of the Li combustion in the event of a Li leak, and is kept at negative pressure to prevent uncontrolled releases of the tritium. However, an air leaks to the Li loop area by the negative pressure. Therefore, the air components leaked to Li loop area are removed by the Ar purification system using a pressure swing absorption (PSA) method. In this process, the exhaust gas (air + Ar purge gas) from the Ar Purification system may be contaminated by tritium remained in the adsorbent bed of PSA. If the tritium from the Li loop area leaks to the exhaust gas of the Ar purification system, the tritium concentration of the exhaust gas become up to 3.5×10^{-2} Bq/cc. Which is larger than 5×10^{-4} Bq/cc of IFMIF design target (1/10 of allowable tritium concentration as water in exhaust gas to atmosphere [6-6]). In this case, the exhaust gas from the Ar purification system has to be processed by the exhaust detritiation system for the tritium contaminated air.

In order to adjust the pressure in the Li loop area, a part of the Ar gas (1 Nm^3/h) purified by the Ar purification system is discharged, and new Ar gas is supplied. For conservative evaluation, it is assumed that the exhaust gas of the Ar purification system does not contain tritium. All tritium permeated from the liquid Li to the Li loop area is processed by the exhaust detritiation system for tritium contaminated Ar, and its concentration becomes 1 Bq/cc. (Which is almost same to the tritium concentration in the Li loop area, and the gaseous tritium in the Li loop area is 1.5×10^{9} Bq.) The design of the exhaust detritiation system for the tritium contaminated Ar does not depend on the tritium permeation from the Li loop, because the tritium permeation rate to the Li loop area is smaller than 6×10^{7} Bq/h [6-7] of the generated tritium in the tritium test module processed by same system.

The permeation rate at the V-Ti hot trap is about 95% of the total tritium permeation rate. Therefore, the reduction of the tritium permeation rate from only the V-Ti hot trap

can directly reduce the total tritium permeation from the Li loop and the gaseous tritium in the Li loop area. For example, if the tritium concentration of the liquid Li into the V-Ti hot trap is reduced by the yttrium hot trap, the permeation rate from the V-Ti hot trap can be reduced. The sum of the tritium permeation rates from the V-Ti hot trap and the heat exchanger is 99 % of the total tritium permeation rate from the Li loop. If they are reduced by two orders of magnitude, the exhaust gas from the Ar purification system can release to atmosphere without tritium removal by the exhaust detritiation system for tritium contaminated air.

The tritium contained in the walls wet by liquid Li in the IFMIF is shown in Fig. 6-4. The amount of total tritium contained in the walls is 5.3×10^{7} Bq, and the tritium contained at the V-Ti hot trap is about 95% of the total tritium contained in the walls wet by liquid Li in the IFMIF. TABLE II shows comparison of deposited tritium in the IFMIF. The amount of the total tritium contained in the walls is much smaller than 4.9×10^{14} Bq of the tritium contained in the liquid Li of 9 m^3 in the IFMIF.

6.5 Summary

The tritium inventory and the permeation of the IFMIF Li loop components are evaluated for the safety of the IFMIF. The amount of total tritium permeation rate is 9.6×10^{5} Bq/h, of which about 95 % is the permeation rate at the V-Ti hot trap. Therefore, the reduction of the tritium permeation rate from only the V-Ti hot trap can directly reduce the total tritium permeation from the Li loop and the gaseous tritium in the Li loop area. The design of the exhaust detritiation system for the tritium contaminated Ar does not depend on the tritium permeation from the Li loop, because the tritium permeation rate from the Li loop is smaller than the tritium from the tritium test module processed by same system. The total tritium contained in the walls wet by liquid Li in the IFMIF is 5.3×10^{7} Bq, and is much smaller than 4.9×10^{14} Bq of the tritium contained in the Li flow with a volume of 9 m^3.

References

[6-1] SAKURAI, T., et al., "Control of nitrogen concentration in liquid lithium by hot trapping," Fusion Eng. Des., **61-62**, 763 (2002).

[6-2] NAKAMURA, H. , et al., "Removal and control of tritium in lithium target for international fusion material irradiation facility (IFMIF)," Fusion Sci. Tech., **41**, 845 (2002).

[6-3] Mueller, W.H., "Metal Hydrides" ,Academic Press, New York, (1968).

[6-4] TANABE, T., et al., "Hydrogen transport in stainless steels", J. Nucl. Mater. **122-123**, 1568 (1984).

[6-5] CRANK, J.,"The Mathematics of Diffusion", Clarendon press, Oxford (1975).

[6-6] ICRP Recommendations, ICRP Publication 60 (1990).

[6-7] T. YUTANI, et al., "Tritium processing and tritium laboratory in the international fusion material irradiation facility (IFMIF)," Fusion Sci. Tech., **41**, 850 (2002).

Table 6-1. Specification of the Li loop components.

Component		Area (m^2)	Thickness (mm)	Temperature (K)
Pipe of Main Loop	From Quench Tank to EMP	5.8	9.3	558
	From EMP to Heat Exchanger	6.4	8.2	558
	From Heat Exchanger to Target	13.5	8.2	523
Quench Tank		7.5	12	558
Target Assembly		1.5	6	523
Heat Exchanger	Pipes for Heat Transfer	444	2.6	523-558
	Outer Wall	27	15	523-558
Pipe between Main and Purification Loops		17	2.8	558
Y Hot Trap	Trap	1.8	8	558
	Pipe	0.76	2.8	558
Cold Trap	Trap	3.3	9	473
	Pipe (to Trap)	0.38	2.8	558
	(from Trap)	0.38	2.8	473
V-Ti Hot Trap	Trap	2.8	15	873
	Economizer(to Trap)	1.2	2.8or3.7	558-723
	(from Trap)	0.29	2.8or3.7	06-873
	Pipe(to Trap)	0.29	2.8	723
	(from Trap)	0.28	2.8	873

Table 6-2. Comparison of deposited tritium.

	Tritium Inventory(Bq)
Tritium in walls wet by Li	5.3×10^{7}
Gaseous tritium in Li loop Area	1.5×10^{9}
Tritium in Liquid Li	5.6×10^{14}

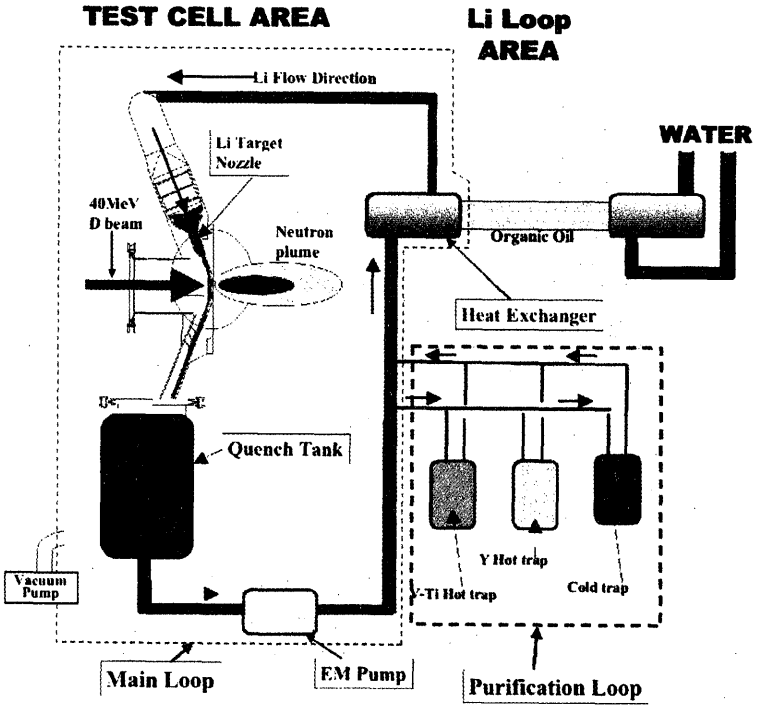

Fig. 6-1. Block diagram of target system of the IFMIF.

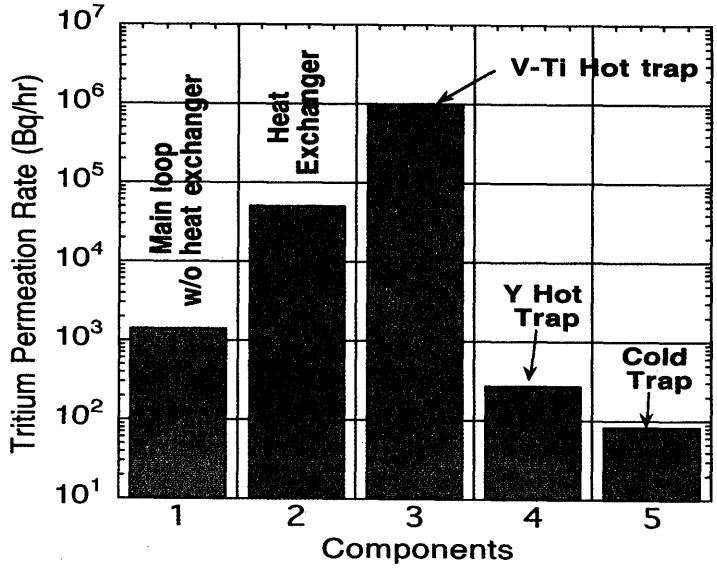

Fig. 6-2. Tritium permeation rate from the Li loop of the IFMIF.

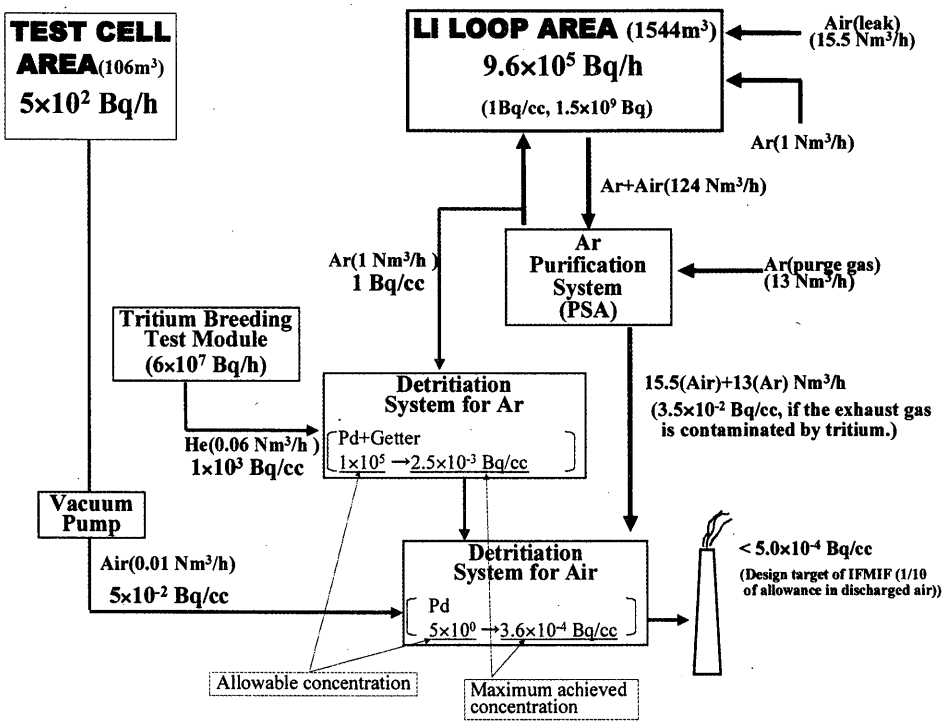

Fig.6-3 Flow chart of the tritium processing for permeated tritium from liquid Li.

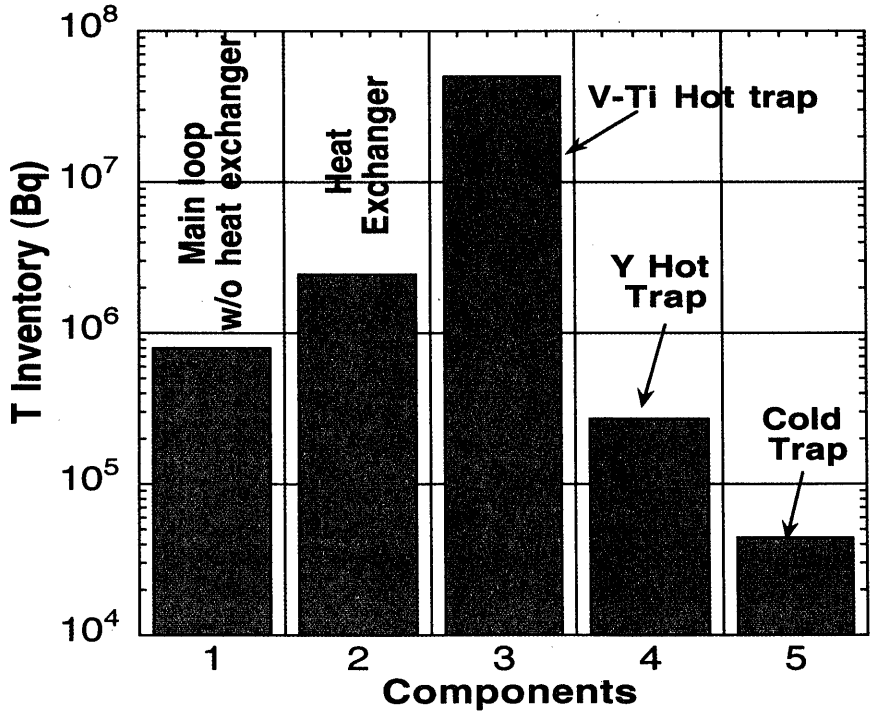

Fig. 6-4. Tritium contained in the walls wetted by liquid Lithium in the IFMIF.

7. Summary

The thermal and thermal-stress analyses of the target assembly revealed that 1) thickness of the thermal shield can be reduced to 20 mm by employing stainless steel with emissivity of 0.05; 2) liquid Li should be charged and circulated under vacuum condition; 3) total required capacity of the heater system would be 14 kW; and 4) the backwall deformation would be reduced from 2 to 0.3 mm by increasing heat transfer coefficient from 15.8 to 150 $W/m^2 \cdot K$.

Activation level of the 316LN stainless steel back wall was estimated to be 3.1×10^{14}, 2.8×10^{14}, 2.3×10^{14} and 7.5×10^{13} Bq/kg after cooling time of 1 day, 1 week, 1 month and 1 year, respectively. After a shut-down, Co-58 with a half-life of 2.33 month is dominant in the total activity for 3 months. After that, Mn-54 and Co-57 become dominant in the total activity. Based on the calculations for radiation dose rate around the Li loop pipe near the electromagnetic pump, hands-on maintenance is possible if fractional deposition (plate-out) of corrosion materials is less than 10% for a permissible level of 10 μSv/hr. Therefore, a removal of radioactive material in Li more than 90 % is needed for the maintenance work.

The total amount of tritium permeation rate through Li loop components was estimated to be 9.6×10^5 Bq/h, of which about 95 % was the permeation through the V-Ti hot trap. Therefore, the V-Ti hot trap is a key component to reduce the total tritium permeation from the Li loop and the gaseous tritium in the Li loop area. The design of the exhaust detritiation system for the tritium contaminated Ar was unnecessary to change because the tritium permeation rate from the Li loop was much smaller than that from the other sources. The total tritium contained in the walls wet by liquid Li was 5.3×10^7 Bq, which was negligibly small compared with the tritium contained in the Li flow with a volume of 9 m^3, 4.9×10^{14} Bq.

Acknowledgements

Appreciation is given to all members of the IFMIF international team on their contributions to this work. The IFMIF executive subcommittee has been highly impressed with dedication and enthusiasm of the IFMIF team. Also, appreciation is given to for the continued interest of the IEA-FPCC and IEA Executive Committee on Fusion Material. Finally, the authors in JAERI are grateful to Drs. M. Seki, S. Seki, H.Takatsu and H.Tsuji for their supports to IFMIF activities.

国際単位系(SI)と換算表

表1　SI基本単位および補助単位

量	名称	記号
長さ	メートル	m
質量	キログラム	kg
時間	秒	s
電流	アンペア	A
熱力学温度	ケルビン	K
物質量	モル	mol
光度	カンデラ	cd
平面角	ラジアン	rad
立体角	ステラジアン	sr

表2　SIと併用される単位

名称	記号
分，時，日	min，h，d
度，分，秒	°，′，″
リットル	l，L
トン	t
電子ボルト	eV
原子質量単位	u

1 eV=1.60218×10^{-19} J

1 u=1.66054×10^{-27} kg

表3　固有の名称をもつSI組立単位

量	名称	記号	他のSI単位による表現
周波数	ヘルツ	Hz	s^{-1}
力	ニュートン	N	$m\cdot kg/s^2$
圧力，応力	パスカル	Pa	N/m^2
エネルギー，仕事，熱量	ジュール	J	N·m
工率，放射束	ワット	W	J/s
電気量，電荷	クーロン	C	A·s
電位，電圧，起電力	ボルト	V	W/A
静電容量	ファラド	F	C/V
電気抵抗	オーム	Ω	V/A
コンダクタンス	ジーメンス	S	A/V
磁束	ウェーバ	Wb	V·s
磁束密度	テスラ	T	Wb/m^2
インダクタンス	ヘンリー	H	Wb/A
セルシウス温度	セルシウス度	℃	
光束	ルーメン	lm	cd·sr
照度	ルクス	lx	lm/m^2
放射能	ベクレル	Bq	s^{-1}
吸収線量	グレイ	Gy	J/kg
線量当量	シーベルト	Sv	J/kg

表4　SIと共に暫定的に維持される単位

名称	記号
オングストローム	Å
バーン	b
バール	bar
ガル	Gal
キュリー	Ci
レントゲン	R
ラド	rad
レム	rem

1 Å=0.1 nm=10^{-10} m

1 b=100 fm^2=10^{-28} m^2

1 bar=0.1 MPa=10^5 Pa

1 Gal=1 cm/s^2=10^{-2} m/s^2

1 Ci=3.7×10^{10} Bq

1 R=2.58×10^{-4} C/kg

1 rad=1 cGy=10^{-2} Gy

1 rem=1 cSv=10^{-2} Sv

表5　SI接頭語

倍数	接頭語	記号
10^{18}	エクサ	E
10^{15}	ペタ	P
10^{12}	テラ	T
10^{9}	ギガ	G
10^{6}	メガ	M
10^{3}	キロ	k
10^{2}	ヘクト	h
10^{1}	デカ	da
10^{-1}	デシ	d
10^{-2}	センチ	c
10^{-3}	ミリ	m
10^{-6}	マイクロ	μ
10^{-9}	ナノ	n
10^{-12}	ピコ	p
10^{-15}	フェムト	f
10^{-18}	アト	a

（注）

1. 表1－5は「国際単位系」第5版，国際度量衡局 1985年刊行による。ただし，1 eVおよび1 uの値はCODATAの1986年推奨値によった。
2. 表4には海里，ノット，アール，ヘクタールも含まれているが日常の単位なのでここでは省略した。
3. barは，JISでは流体の圧力を表わす場合に限り表2のカテゴリーに分類されている。
4. EC閣僚理事会指令ではbar，barnおよび「血圧の単位」mmHgを表2のカテゴリーに入れている。

換算表

力

N(=10^{5}dyn)	kgf	lbf
1	0.101972	0.224809
9.80665	1	2.20462
4.44822	0.453592	1

粘度　1 Pa·s(N·s/m^2)=10 P(ポアズ)(g/(cm·s))

動粘度　1 m^2/s=10^{4}St(ストークス)(cm^2/s)

圧力

MPa(=10 bar)	kgf/cm^2	atm	mmHg(Torr)	lbf/in^2(psi)
1	10.1972	9.86923	7.50062×10^3	145.038
0.0980665	1	0.967841	735.559	14.2233
0.101325	1.03323	1	760	14.6959
1.33322×10^{-4}	1.35951×10^{-3}	1.31579×10^{-3}	1	1.93368×10^{-2}
6.89476×10^{-3}	7.03070×10^{-2}	6.80460×10^{-2}	51.7149	1

エネルギー・仕事・熱量

J(=10^{7}erg)	kgf·m	kW·h	cal(計量法)	Btu	ft·lbf	eV
1	0.101972	2.77778×10^{-7}	0.238889	9.47813×10^{-4}	0.737562	6.24150×10^{18}
9.80665	1	2.72407×10^{-6}	2.34270	9.29487×10^{-3}	7.23301	6.12082×10^{19}
3.6×10^6	3.67098×10^5	1	8.59999×10^5	3412.13	2.65522×10^6	2.24694×10^{25}
4.18605	0.426858	1.16279×10^{-6}	1	3.96759×10^{-3}	3.08747	2.61272×10^{19}
1055.06	107.586	2.93072×10^{-4}	252.042	1	778.172	6.58515×10^{21}
1.35582	0.138255	3.76616×10^{-7}	0.323890	1.28506×10^{-3}	1	8.46233×10^{18}
1.60218×10^{-19}	1.63377×10^{-20}	4.45050×10^{-26}	3.82743×10^{-20}	1.51857×10^{-22}	1.18171×10^{-19}	1

1 cal = 4.18605 J(計量法)

= 4.184 J（熱化学）

= 4.1855 J（15 °C）

= 4.1868 J(国際蒸気表)

仕事率　1 PS(仏馬力)

= 75 kgf·m/s

= 735.499 W

放射能

Bq	Ci
1	2.70270×10^{-11}
3.7×10^{10}	1

吸収線量

Gy	rad
1	100
0.01	1

照射線量

C/kg	R
1	3876
2.58×10^{-4}	1

線量当量

Sv	rem
1	100
0.01	1

（86年12月26日現在）

Review of JAERI Activities on the IFMIF Liquid Lithium Target in FY2004